University of Stavanger

Faculty of Science and Technology

MASTER'S THESIS

Study program/Specialization: Petroleum Engineering – Drilling Engineering	Spring semester, 2017 <u>Open</u> / Restricted access
Writer: Bendik Følling	…… (Writer's signature)
Faculty supervisor: Dan Sui External supervisor(s):	
Thesis title: Experimental Study on Automatic Evaluation of Drilling Fluid Properties	
Credits (ECTS): 30	
Key words: - Automation - Drilling fluid properties evaluation - Flow loop - Experimental - Drilling hydraulics	Pages: 73 + enclosure: 14 Stavanger, 14/06-2017 Date/year

Master's Thesis

Experimental Study on Automatic Evaluation of Drilling Fluid Properties

Bendik Følling

Faculty of Science and Technology
University of Stavanger

This thesis is submitted for the degree of
Master of Science

June 2017

Acknowledgements

This thesis concludes my studies as a masters student in Petroleum Technology at the University in Stavanger.

I would like to thank my supervisor, Dan Sui, for being available for discussions through the whole semester and for being helpful with the Matlab™- codes used in the thesis. I would also like to thank Jostein Djuve for support in the drilling fluid laboratory and Hydrawell for the fluid addititves.

Finally, I want to thank my family, friends and fellow students for all support and five great years at the University.

Abstract

The drilling fluid has several important functions such as transporting cuttings out of the well and being a primary barrier during the drilling operation. When drilling challenging wells in the present and future, factors like safety, time and cost efficiency are important to consider. A system that could deliver live data of fluid density and viscosity in the well would improve the bottom hole pressure control, and further help to save time and avoid fatal accidents.

The instrumented standpipe concept evaluated in this thesis can potentially deliver improved bottom hole pressure control to the drilling crew by estimating density and viscosity in real time.

Last year, a flow loop was constructed in the drilling hydraulics laboratory as a bachelor thesis to evaluate the instrumented standpipe concept. This thesis is a thorough experimental test of the flow loop and its potential to deliver stable live data of density and viscosity. Horizontal and vertical differential pressure are used to estimate density and viscosity of both Newtonian and non-Newtonian fluid in laminar and turbulent flow regime.

The test results indicated inaccurate differential pressure readings at first. After calibrating the flow loop with water and adding an offset correction to the differential pressure, the system proved good results both for Newtonian and non-Newtonian fluids.

The flow loop still needs some further modifications. Pressure sensors should be exchanged to give more reliable data. Different fluid mixes should also be tested.

Table of contents

List of figures

List of tables

Nomenclature

Symbols

$\dot{\gamma}$	Shear rate
$\dot{\gamma}_w$	Shear rate at wall
ε	Absolute pipe roughness
μ_a	Apparent viscosity
ρ	Fluid density
τ	Shear stress
τ_w	Shear stress at wall
τ_y	Yield stress
θ	Measured angle [°] in degrees
ΔL	Length of pipe between pressure sensors
ΔP	Differential pressure drop
$\Delta P_{friction}$	Frictional pressure drop
A	Inner cross-sectional pipe area
D	Inside diameter of pipe
D_{eff}	Effective inner diameter of pipe
dP_{hor}	Differential pressure in horizontal section
dP_{ver}	Differential pressure in vertical section

f	Darcy-Weisbach friction factor
g	Gravitational constant [9,81 m/s^2]
h	Height between pressure sensors in vertical section
K	Consistency index
L	Length of pipe between pressure sensors
m	Generalized flow index
n	Flow index
n_a	Generalized flow index
P	Hydrostatic pressure
Q	Flow rate
Re	Reynolds number
Re_{HB-gen}	Generalized Herschel Bulkley Reynolds number
u	Fluid velocity $[m/s]$

Abbreviations

AV	Apparent viscosity
BHP	Bottom hole pressure
cP	Centipoise
ECD	Effective circulation density
$g/liter$	gram/liter
HB	Herschel Bulkley
$mBar$	10^{-3} Bar
OBM	Oil based mud
Pa	Pascal
PAC	Polyanionic Cellulose

PID	Proportional, Integral, Derivative
ROP	Rate of penetration
RPM	Rounds per minute
SG	Specific Gravity
WBM	Water based mud

Chapter 1

Introduction

1.1 Background

The drilling fluid has severe importance during drilling operations, and has several functions such as lubricator for the drill string and drill bit. Other functions are transporting cuttings out of the well and hold the cuttings suspended in the fluid when the drilling fluid pump is shut off.

However, its most crucial function is to provide pressure control of the well. It is therefore important to monitor the fluid during operation to ensure that the fluid has the right composition of additives for the section being drilled, and to make sure the hydrostatic pressure provided by the fluid is within the safe operational window between the formations collapse and fracturing pressure gradients. If the bottom hole pressure (BHP) provided by the drilling fluid drops below the formation pore pressure during operation, formation fluid will enter the well, causing a kick. For BHP higher than the fracturing pressure, the formation fractures and the drilling fluid will be lost into the formation, causing a decreased hydrostatic pressure. Both scenarios can lead to a kick and in worst case a blow out.

Density and viscosity of the fluid are being monitored at the drilling facility. By monitoring the fluid density, influxes of formation fluid and fluid loss to formation can be detected relatively fast and potential accidents can be avoided. Viscosity is being monitored as it regulates the efficiency of cuttings transport out of the well. The frictional pressure drop in annulus and drill pipe is also dependent on the viscosity. Together, viscosity and density regulates the effective circulation density (ECD) against the formation, where ECD equals the fluid density plus the added frictional pressure drop in the well divided by the gravitational constant and depth.

Today the standard procedure for measuring density and viscosity is to take a sample from the return fluid with specified intervals. By using a mud balance scale, the density in the

well can be measured and by using a Marsh Funnel the effective viscosity can be established. Apparent viscosity can be estimated with the use of a Fann®35 viscometer or similar.

In this thesis we will evaluate the instrumented standpipe concept with the use of a flow loop that was built in the drilling hydraulics laboratory in 2016. By continuously measuring the differential pressure drop of the fluids in the horizontal and vertical pipe of the flow loop, density and viscosity data can be estimated and read from the computer screen in 'real time'.

1.2 Motivation

In the Petroleum industry; safety, time efficiency and cost reduction have been main focus areas during the low oil price the last years.

The motivation behind this thesis is to evaluate the instrumented standpipe model's accuracy, as it can deliver improved safety and well control with live measurements of density and viscosity of the drilling fluids. Live data of the pressure drop can observe a change in density in real time, and reduce the risk for an accident. With this concept as a standard, it could also improve the time efficiency and reduce costs as there would be a reduction of the rig crew without the physical testing of the fluid.

1.3 Structure of thesis

The next chapter presents drilling fluid theory and frictional pressure drop calculation methods for Newtonian and non-Newtonian fluid.

In chapter 3 the instrumented standpipe concept is presented. This chapter also includes a summary of how the flow loop was constructed one year ago.

Chapter 4 presents the theory used to estimate density and apparent viscosity for Newtonian and non-Newtonian fluid based on differential pressure measurements done with the flow loop.

Chapter 5 includes a summary of the experimental work and presents the results achieved from the laboratory. These results are further discussed in chapter 6.

In chapter 7 the concluding remarks and recommended future work are presented.

Chapter 2

Fundamentals of drilling fluid technology

This chapter includes theory regarding drilling fluid functions, composition and properties that are relevant for this thesis. It also includes testing procedures of drilling fluid and frictional pressure drop calculation methods that will be further used in chapter 4 and 5.

2.1 Functions of the drilling fluid

The two most important functions of the drilling fluid is to;

1) Remove cuttings below the bit

2) Transport cuttings from drill bit to the surface

A high flushing effect is required to avoid accumulation of cuttings in the bore hole. By inserting small jet nozzles in the drill bit, a sufficient flushing effect called jetting force will be achieved due to a large pressure drop over the nozzles. Up to 50 % of the pressure loss in the mud circulation system is located at the bit through the nozzles [7]. The remaining pressure loss is a result of friction inside the drill string and frictional pressure loss in annular space between bore hole wall and the drill string.

Maintaining a stable well bore and the ability to control formation pressure are two other important functions of the drilling fluid. The right composition of fluid is also necessary for filtration control and to prevent unfortunate chemical- and mechanical damages in the well bore.

Other tasks that the drilling fluid is designed for[7]:

- Lubricate drill string and cool the bit
- Bring information up to surface

- Seal permeable formations
- Minimize reservoir damage
- Transmit hydraulic energy to bit
- Control corrosion
- Minimize damage on environment
- Prevent gas hydrate formation

2.2 Composition of drilling fluids

Drilling fluids, often referred to as drilling mud or mud, is a suspension of solids (e.g. clays, barite, small cuttings) with chemical additives, required to modify properties in any of the liquids described below. Drilling mud can be categorized according to their base fluid [1].

- Water-based mud (WBM): Solid particles are suspended in water or brine. Water is in continuous phase, but oil may be emulsified.
- Oil-based mud (OBM): Solid particles are suspended in oil. Water or brine may be emulsified, while oil is in continuous phase
- Gas: Cuttings are removed by a high velocity stream of air or natural gas. Minor inflows of water are blocked by adding foaming agents

2.3 Properties of the drilling fluid

2.3.1 Density

Density is defined as weight per unit volume and can be expressed as kilograms per cubic meter (kg/m^3), pounds per gallon (lb/gal), pounds per cubic foot (lb/ft^3) or as specific gravity (SG), compared to a equal volume of water.

The hydrostatic pressure in a well generated by the mud column is dependent on mud density and depth. It is therefore convenient to express density as a depth dependent parameter such as pounds per square inch per foot (psi/ft) or kilograms per square centimeter per meter ($kg/cm^2/m$)[1]. To create a thin filter cake and protect the well against inflow of formation fluid, it is important that the hydrostatic pressure of the mud column exceeds

the pore pressure in the formation (with a minimum of 200 psi)[1]. However, in case of excessive mud density, the pressure on the bore hole wall may exceed the natural fracturing pressure of the formation being drilled. The result of this is failure in tension on the bore hole, called induced fracturing. As both pore pressure and fracturing pressure increases with depth, the drilling fluid density will be adjusted several times while drilling the well. To avoid bore hole failure when adjusting the drilling fluid density, the overlaying well section is protected by installing casings. Other disadvantages of excessive mud weight are decreased drilling rate (ROP), increased risk of drill string sticking due to high overbalance pressure and unnecessarily high mud costs[1].

2.3.2 Viscosity

Laminar flow in a circular pipe may be visualized as extremely thin cylinder layers sliding over each other. When two layers of fluid and a solid moves relative to each other, the slower one will decrease the velocity of the faster layer due to friction forces. This internal resistance to flow is called viscosity, which is a measure of internal stickiness of the fluid [2]. All fluids have some degree of viscous effects. Oil and bentonite drilling fluids are of the more viscous fluids, while water has relatively low viscosity.

The difference in velocity between two cylinders, divided by the distance between them, represents the shear rate. Shear stress is defined as axial force divided by the surface area of a cylinder. The ratio of shear stress to shear rate represents the viscosity of the fluid, which has the unit poise or Pa.s. The most common form for viscosity in drilling mud is centipoise(cP), which is one hundredth of a poise or one thousand Pa.s (1 cP = 0,001 Pa.s)

Different flow models can be identified by plotting shear stress versus shear rate. For instance, a linear correlation is defined as a Newtonian fluid. Viscosity for a Newtonian fluid can therefore be calculated from a single shear rate, and be used in hydraulic calculations for any other shear rate[1].

Suspensions such as drilling muds are fluids containing particles larger than molecules in large quantities. These do not behave after the Newtonian law and are often referred to as non-Newtonian fluids and the shear stress/shear rate relationship depends on the composition of the fluid. Clay muds with high solid contents is often referred to as a typical example of a Bingham plastic fluid where a certain shear stress is necessary to initiate flow. This is referred to as the yield point. For shear stresses above this limit, the fluid will behave as a Newtonian fluid. A Bingham fluid is therefore described by two parameters, yield point and plastic viscosity[1].

The shear stress divided by the shear rate is known as the effective or apparent viscosity. If the apparent viscosity of a drilling mud decreases as a result of increased shear rate, which

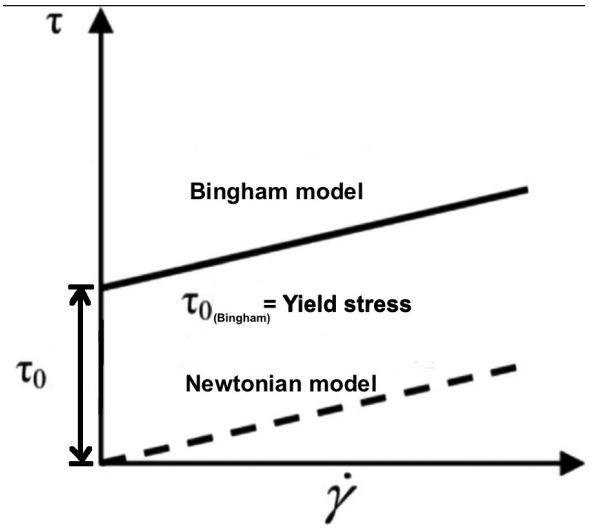

Fig. 2.1. Bingham model

is preferable when drilling, the fluid is *shear thinning*. When the effective viscosity decreases for higher shear rates prevailing in the drill pipe, required pump pressure is reduced. For low shear rates prevailing in the annulus, the viscosity stays relatively high, thus increasing the cuttings carrying capacity [1].

Drilling muds consisting of polymers and little to no solids, behave as they have a yield point for high shear rates, but actually the flow model passes through the origin. These fluids are pseudo-plastic fluids and can be described by the power law, which states that

$\tau = K(\dot{\gamma})^n$

Where τ is shear stress and $\dot{\gamma}$ is shear rate. The parameter K is the shear strength at a shear rate of 1 sec^{-1}, which corresponds approximately to the yield point[1], and n is a measure of the rate of change of viscosity with the shear rate. For a Newtonian fluid, n = 1, and for a shear thinning fluid, n < 1. The lower the value of n, the greater the shear thinning.

When the flow velocity exceeds a certain value, the flow behavior in a pipe changes from laminar to turbulent. Turbulent flow changes locally in velocity and direction and is no longer considered as thin layers sliding over each other. The overall fluid direction of a turbulent flow is still parallel to the axis of the pipe [1].

The critical velocity for when a laminar flow changes to turbulent decreases with increase in pipe diameter, with increase in density and with decrease in viscosity, and is expressed by a dimensionless number known as the Reynolds number [1]. The flow behavior of the drilling fluids usually changes from laminar to turbulent for a Reynolds number between 2000 and 3000. The $Fanning friction factor$ can be calculated from the Reynolds number if given the roughness of the pipe wall.

2.4 Conventional testing of drilling fluid

Having control over the fluid in the well is of up-most importance while drilling. The industry standard today is to take samples from the returning fluid to check the properties of the drilling mud. Simple tests are performed to verify density, viscosity and gel strength of the fluid.

2.4.1 Determination of drilling fluid density

The drilling fluid density is determined by weighing a certain amount of fluid and divide by the precise volume. The density can easily be found by the use of a mud balance scale. Both standard scales and pressurized scales can be used.

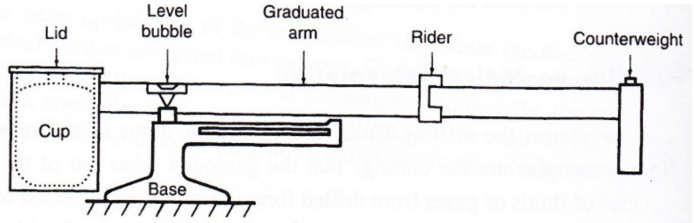

Fig. 2.2. Mud balance scale [Klempa et al.]

Mud is filled to the top of the cup with a lid placed on top. The lid has a small hole in the center which leads excessive mud out of the cup. It is important to wipe of excessive mud to get correct density. The rider is moved along the rod until the level bubble is in center. The density can then be read of on the left side of the rider on the graduated arm.

Density can be expressed in pounds per gallon (lb/gal), pounds per cubic foot (lb/ft^3), grams per cubic centimeter (g/cm^3) or as a gradient of pressure exerted by depth [1].

2.4.2 Determination of viscosity

The viscosity is usually determined by the use of a Marsh Funnel or a direct indicating viscometer. The Marsh Funnel instrument (Fig. 2.3 a) is useful on the drilling facility where it enables the drilling crew to periodically test and detect if sudden changes happens to the consistency of the drilling mud. The instrument consists of a funnel and a measuring cup. Mud is filled into the funnel until it touches a screen and the time it takes for all the fluid to flow from the cone to the measuring cup is measured. The measured time represent the effective viscosity at the rate of shear prevailing in the orifice and partly the rate of gelation[1].

Direct indicating viscometers are a form of concentric cylinder viscometer that enable the variation of shear stress with shear rate to be observed. In the drilling fluid laboratory at UiS, a model called Fann 35 is used, and it allows us to use the following shear rates: 600, 300, 200, 100, 6 and 3 RPM (rounds per minute). The direct indicating viscometers is build up with a bob suspended from a spring and an outer cylinder which can rotate with a constant speed corresponding to the shear rates mentioned above. A cup with mud is elevated upwards the cylinder and tightened when it reaches a specific mark. The viscous drag from the mud turns the bob until it's balanced by the torque in the spring. The deflection of the bob is read from a calibrated dial on top of the instrument, which thus provides a measure of the shear stress at the surface of the bob [1]. The Fann 35 viscometer will be used in the practical part of this thesis.

(a) Marsh Funnel [Wikipedia] **(b)** Fann®35 viscometer [Ru]

Fig. 2.3. Viscosity measurement equipment

2.5 Frictional pressure drop calculations

2.5.1 Pressure drop calculations for Newtonian fluid

Fluids that flows in a pipe experience frictional forces due to friction against pipe wall and friction between particles in the fluid. The pump pressure has to overcome the horizontal frictional pressure drop that the fluids experience, for the fluid to obtain flow in a horizontal

direction. The pressure drop between two points, P1 and P2, can be calculated from the *Darcy – Weisbach* equation:

$$\Delta P = \frac{fL\rho u^2}{2D} \tag{2.1}$$

Here, ΔP is the pressure loss, f is Darcy-Weisbach friction factor, L is length of pipe between the pressure measurements, ρ is the fluid density, D is the inner pipe diameter and u is the average velocity, which can be determined from Equation (2.2).

$$u = \frac{Q}{A} \tag{2.2}$$

Where Q is the flow rate and A is the inner cross section area of the pipe.

The Darcy-Weisbach friction factor for Newtonian fluid is calculated different for laminar and turbulent flow, and Reynolds number is necessary to describe the flow regime. For Reynolds number less than 2300 the flow is usually considered to be laminar. Reynolds number between 2300 and 4000 refers to a transition phase flow regime, and a Reynolds number above 4000 is considered to refer to a turbulent flow regime. However, the critical Reynolds number will not be the same for every system. For laminar flow, the Reynolds number can be calculated as in Equation (2.3).

$$Re = \frac{\rho u D}{\mu} \tag{2.3}$$

Further, the friction factor can be calculated from Equation (2.4), while various equations can be used for turbulent flow. In this thesis, Haaland's equation (Equation (2.5)) is used for turbulent flow [5].

$$f = \frac{64}{Re} \tag{2.4}$$

$$\frac{1}{\sqrt{f}} = -1.8log\left[\left(\frac{\varepsilon/D}{3.7}\right)^{1.11} + \frac{6.9}{Re}\right] \tag{2.5}$$

It is important that the inner pipe diameter, D, and the absolute roughness of the pipe, ε, has the same dimensions when using Haaland's equation.

With f, ε, D, Re, ρ and Q known, the fluids pressure loss due to friction can be calculated by using Equation (2.1).

2.5.2 Herschel Bulkley model

The Herschel Bulkley model is basically a combination of the Power law model and Bingham plastic model, where a minimum shear force is required to initiate flow. Once the fluid is viscous, it will behave according to the Power law, where the shear stress to shear rate relationship describes a shear thinning liquid [1].

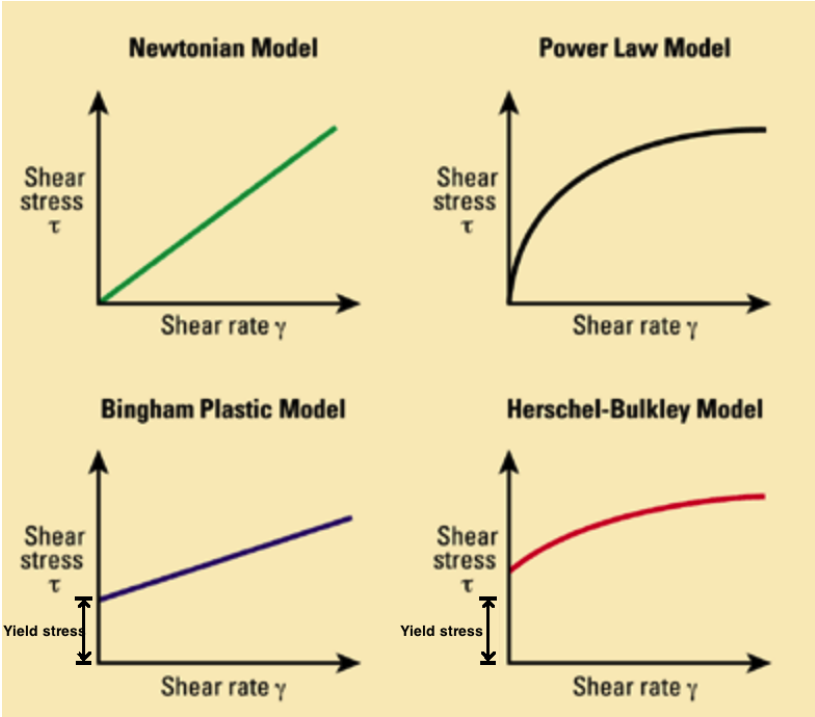

Fig. 2.4. Herschel Bulkley in the lower right corner [Glossary]

This model will be used as it fits the Fann®35 data best. The Herschel Bulkley model can be explained with Equation (2.6).

$$\tau = \tau_y + K(\dot{\gamma})^n \tag{2.6}$$

Where, τ - Shear stress $[Pa]$, τ_y - Yield stress $[Pa]$, K - Consistency index, $\dot{\gamma}$ - Shear rate $[s^{-1}]$, and n - Flow index

The Herschel Bulkley model describes fluids with shear thinning properties ($n < 1$), where n can be calculated from equation (2.7).

$$n = \frac{log(\frac{\theta_{600}-\theta_0}{\theta_{300}-\theta_0})}{log(\frac{1022}{511})} \tag{2.7}$$

Here, θ is measured angle [°] in degrees read of the Fann®35 at one of the given rotational frequencies, RPM (rounds per minute). At 0 RPM, the shear stress is impossible to measure. It is therefore estimated with equation (2.8) [3].

$$\theta_0 = 2 \cdot \theta_3 - \theta_6 \tag{2.8}$$

When n is calculated, it can be used to determine the consistency index, K, by using Equation (2.9)

$$K = 0.511 \cdot (\frac{\theta_{600} - \theta_0}{1022^n}) \tag{2.9}$$

The yield stress, τ_y $[Pa]$, is the minimum shear force needed to initiate flow to the fluid, and can be estimated by Equation (2.10).

$$\tau_y = 0.511 \cdot \theta_0 \tag{2.10}$$

Further, by using the RPM and a converting factor, Equation (2.11), the shear rate, $\dot{\gamma}$, can be estimated.

$$\dot{\gamma} = RPM \cdot 1.7023 \tag{2.11}$$

Finally, the apparent viscosity can be estimated with Equation (2.12).

$$\mu_a = \frac{\tau}{\gamma} \tag{2.12}$$

Where μ_a is in $[Pa \cdot s]$. To convert to $[cP]$, multiply Equation (2.12) by 1000.

2.5.3 Pressure drop calculation for non-Newtonian fluid

For the non-Newtonian fluid pressure drop calculation, K. Madlener, B. Frey and H.K. Ciezki presented a way to calculate the generalized Hershel Bulkley (HB) Reynolds number for all flow regimes for non-Newtonian fluids, with viscosity characteristics following the HB equation [9].

$$Re_{HB-gen} = \frac{\left(\rho u^{2-n} D^n\right)}{\left(\frac{\tau_y}{8}\left(\frac{D}{u}\right)^n + K\left(\frac{3m+1}{4m}\right)^n 8^{n-1}\right)} \tag{2.13}$$

Where

$$m = \frac{nK(8u/D)^n}{\tau_y + K(8u/D)^n} \tag{2.14}$$

Here, m is the generalized flow index. Further, the effective inner diameter off the pipe for non-Newtonian flow is expressed in the following equation:

$$D_{eff} = \frac{4m}{3m+1} \tag{2.15}$$

For laminar flow, equation (2.4) with the generalized HB Reynolds number is used to calculate the friction factor, while the transient and turbulent flow uses a modified version of Haaland's equation, presented in equation (2.9).

$$\frac{1}{\sqrt{f}} = -1.8log\left[\left(\frac{\varepsilon/D_{eff}}{3.7}\right)^{1.11} + \frac{6.9}{Re_{HB-gen}}\right] \tag{2.16}$$

Finally, the pressure drop can be calculated as follows when the fluid density is known.

$$\Delta P = \frac{fL\rho u^2}{2D_{eff}} \tag{2.17}$$

The apparent viscosity can be calculated by Equation (2.18)

$$\mu_a = \frac{\rho u D_{eff}}{Re_{HB-gen}} \tag{2.18}$$

Chapter 3

Automatic evaluation of drilling fluid properties

This chapter includes theory for the instrumented standpipe concept and a short description of how the flow loop was constructed.

3.1 Instrumented standpipe concept

The idea behind the instrumented standpipe concept is to use differential pressure sensors to get real time data values for the density and viscosity of the fluid [12]. Pressure sensors are installed as seen in the illustration below, with two sensors on the horizontal pipe and two on the vertical pipe.

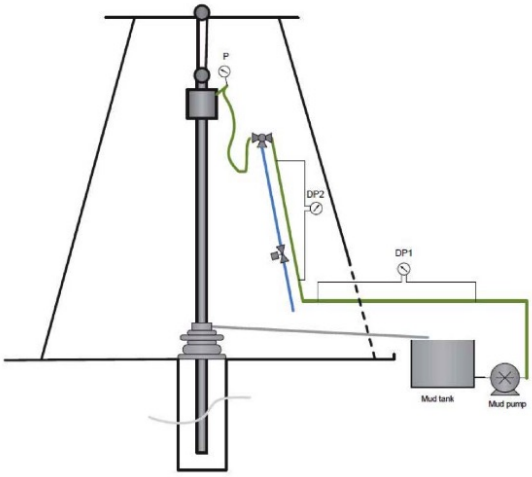

Fig. 3.1. Illustration of the standpipe concept [12]

In the picture, DP1 is the horizontal differential pressure between sensor 1 and 2, while DP2 is the vertical differential pressure between sensor 3 and 4. From this point, DP1 will be referred to as dP_{hor} (horizontal) and DP2 will be referred to as dP_{ver} (vertical). There is no hydrostatic pressure in the horizontal section, hence the pressure loss between sensor 1 and 2 corresponds to friction in the pipe only. In the vertical section, pipe diameter, pipe roughness and length between the sensors are the same as for horizontal. The frictional pressure drop should therefore be the same for vertical section as for the horizontal, when assuming equal flow behavior. However, the largest part of the differential pressure in the vertical part, dP_{ver}, corresponds to the hydrostatic pressure drop.

3.2 Flow loop description

Last year a flow loop was constructed as a bachelor thesis with the purpose of evaluating the instrumented standpipe concept.

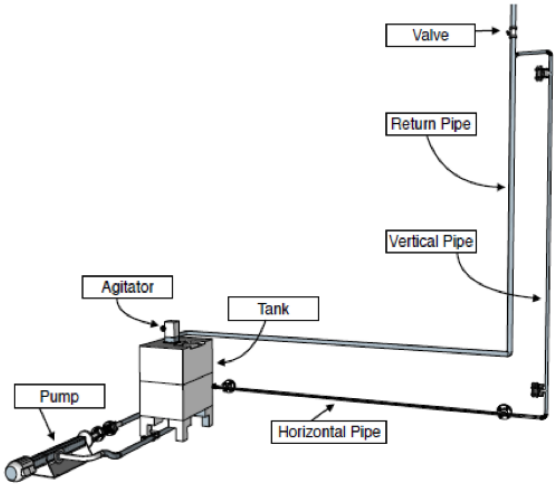

Fig. 3.2. Sketch of the flow loop [6]

The horizontal and vertical pipes shown in Fig. 3.2 is made of plastic with an inner diameter of 24mm, while the return pipe has a diameter of 50 mm.

All pipes are transparent and have a smooth inner surface. In corners and pipe connections, gray PVC fittings were used. Two pressure sensors are mounted on a T-bar with a distance of 3.5 meter for both horizontal and vertical pipe. Differential pressure transmitters are connected to the sensors[6].

The tank is made out of plastic and can contain up to 200 liters. It has an elevated support structure and a conical bottom. An agitator is placed on top of the tank for the possibility to

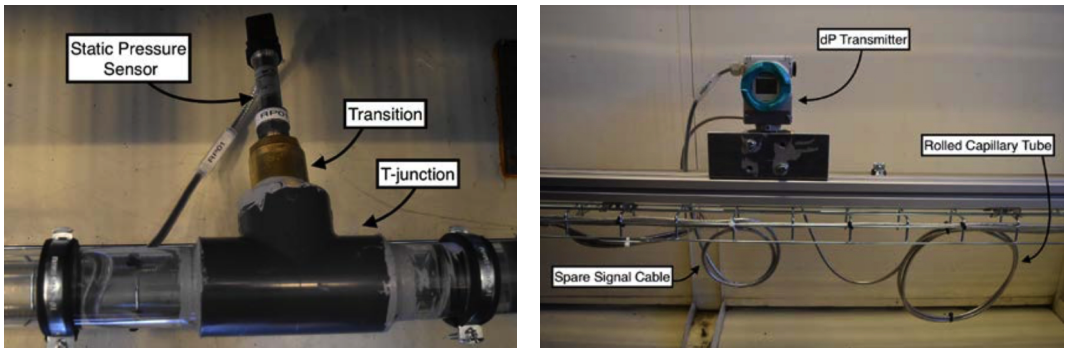

(a) Pressure sensor [6] **(b)** dP Transmitter [6]

Fig. 3.3. Pressure sensor and dP transmitter

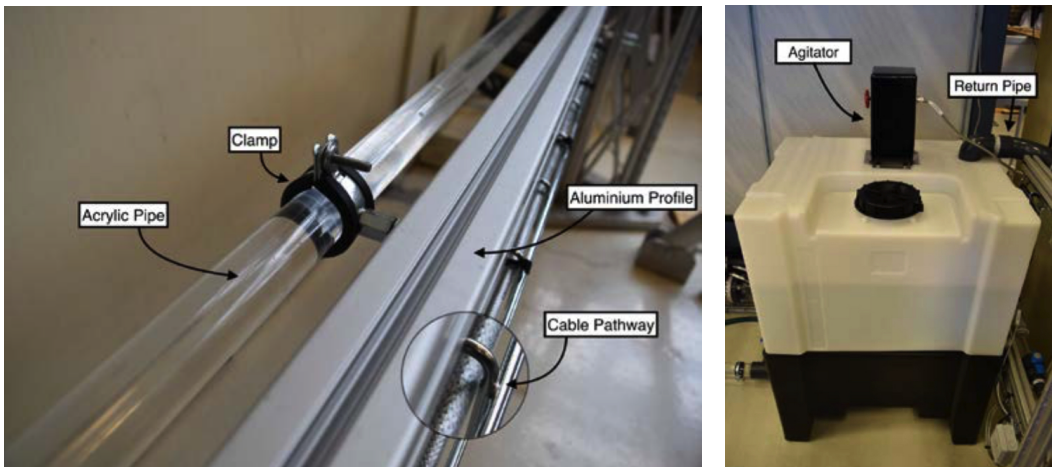

(a) Acrylic pipe with 24 mm diameter [6] **(b)** 200 liter tank [6]

Fig. 3.4. Flow loop pipes and tank

stir the fluid. A temperature sensor and a level switch is mounted on the right wall of the tank, while the return pipe's outlet is placed in the top corner of the tank. If the water level is too low, the level switch will shut down the pump.

A mono progressive cavity pump, type C1XKS81RMA was chosen based on the following criteria [6]:

- Must be able to pump at low flow rates, even at high pressures
- Relatively low pressure pulses
- Purely positive displacement of the fluid
- Positive experiences from past laboratory projects
- The pump house needed to be made of Maritime Stainless Steel(SAE 316)

All the electrical cables in the fuse box was connected by a third year electro engineer that co-worked with the two petroleum engineers on the bachelor thesis. A second cabinet containing a frequency converter is placed between pump and tank. The frequency converter is used to accurately regulate the speed of the pump, thus controlling the flow rate of the fluid in the flow loop. A flow-meter is also installed at the outlet of the pump

Fig. 3.5. Flow meter with display [6]

A communication card was installed in order to communicate between the different sensors and the computer. For this rig they chose the NI PCIe- 6321 Multifunction Data Acquisition Device with 2 two analog outputs, 16 analog inputs and 24 digital input/output channels [6].

Table 3.1. Input signal

Horizontal dP sensor	Analog
Vertical dP sensor	Analog
Pressure sensor	Analog
Temperature sensor	Analog
Electromagnetic flow meter	Analog

Table 3.2. Output signal

Pump set-point	Analog
Pump on/off	Digital
Agitator on/off	Digital

Flowchart of the data acquisition is shown in (fig 3.7)

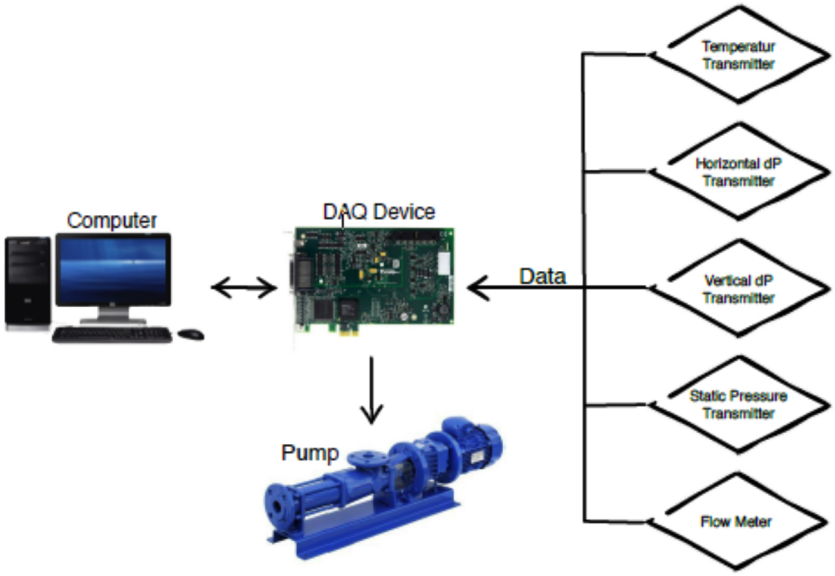

Fig. 3.6. Data acquisition system [6]

3.3 Simulink

A part of the Simulink structure is illustrated in Fig. 3.7. Pump set-point in the upper left corner is set 8 l/min in the figure. Since the pump is driven by electricity, a saturation block is added to the Simulink structure to convert frequency (Hz) into required flow rate.

The PID block was added to the structure during the experimental testing in this thesis, with the intention of improving the flow rate accuracy. PID stands for Proportional, Integral, Derivative and the PID controller is the most widely used controller in modern industry. The PID-controller is used in more than 95% of all closed-loop industrial processes, even though you find controllers today that are a lot more advanced [12]. By adjusting the controller gain parameters K_p, K_i and K_d in the PID controller, desired flow rate can be reached earlier with smaller pulsations.

- K_p is used to decrease the rise time
- K_i is used to eliminate the offset
- K_d is used to reduce overshoot and settling time

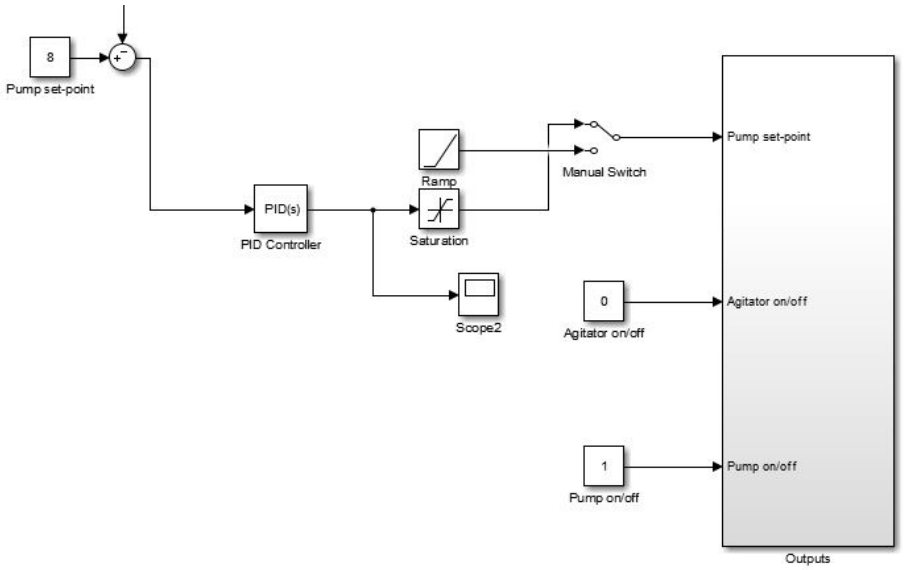

Fig. 3.7. Layout

Figure 3.8 illustrates how the low pass filter is added to the raw measurements while the flow loop is running. Different variations of the low pass filter below were tested during the calibration of flow loop

$$\frac{1}{\alpha s+1}$$

The low pass filter blocks provided by Simulink, shown in figure 3.8, was permanently used in chapter 5 for all sampled measurements.

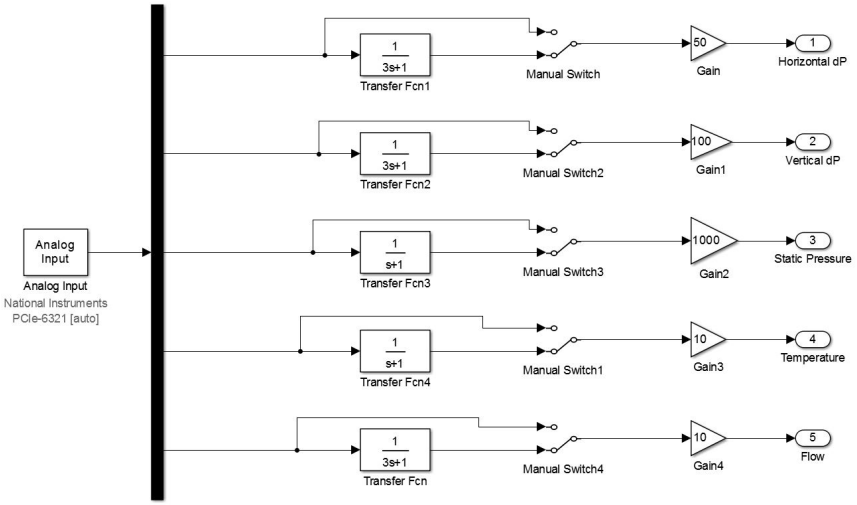

Fig. 3.8. Low pass filter

Chapter 4

Calculation Methods for the Flow Loop

This chapter introduces calculation methods used in the experimental part, chapter 5. Newtonian and non-Newtonian fluids behave different during flow when it comes to viscosity, the ability to flow. Chapter 4.1 will present the standard calculation method for viscosity and density for Newtonian fluids, while chapter 4.2 will present the Herschel Bulkley model for non-Newtonian fluids and the Rabinowitsch-Mooney equation.

4.1 Newtonian fluid

Still water parameters in room temperature are well known and will be used to calibrate the flow loop, shown in chapter 5.

Newtonian fluid viscosity has a linear relationship between shear stress and shear rate, and the flow model (also known as consistency curve) passes through origin. Since Newtonian fluids does not change with shear rate, hydraulic calculations can be carried out for flow at any shear rate.

The actual apparent viscosity for room temperated water is 1 cP and the density is usually said to be 1000 kg/m^3. By running the flow loop and knowing these parameters, the system can be calibrated and later be used when adding Xanthan gum to the water.

Calculation method for fluid properties when running the flow loop is shown in the sub-chapters below.

4.1.1 Density

Hydrostatic pressure can be used to calculate the density when assuming that the frictional pressure drop is the same for ΔL in both horizontal and vertical section.

$$P = \rho g h \tag{4.1}$$

Here h is L, the vertical distance between the sensors. Solving Equation (4.1) with respect to the fluid density, ρ, we get

$$\rho = \frac{P}{gL} \tag{4.2}$$

Since the distance L between the horizontal pressure sensors and L between the vertical sensors are the same, dynamic pressure loss should also be the same. Considering this, the density can be estimated with Equation (4.3).

$$\rho = \frac{dP_{ver} - dP_{hor}}{gL} \tag{4.3}$$

Where $dP_{ver} - dP_{hor}$ represents the hydrostatic pressure for all flow rates, g is the gravitational constant, and L is the distance between the vertical pressure sensors.

4.1.2 Darcy-Weisbach Friction Factor

The Darcy-Weisbach friction factor can be solved from rearranging Equation (2.1), as shown below.

$$f = \frac{dP_{hor} \cdot 2D}{\rho L u^2} \tag{4.4}$$

Where, dP_{hor} is measured pressure loss in the horizontal pipe between the sensors, ρ is the calculated density, L is the length between the pressure measurement points, u is the average fluid velocity, solved from Equation (2.2), and D is the inner pipe diameter.

4.1.3 Reynolds Number

When the friction factor is estimated, Reynolds number can be calculated, both for laminar and turbulent flow. In this thesis laminar flow is assumed when Re < 2000, while for Re > 2000 the flow regime is assumed turbulent.

Laminar flow

Solving Equation 2.4 with respect to *Re*, we get

$$Re_{lam} = \frac{64}{f} \tag{4.5}$$

Turbulent flow

Solving Equation (2.5) with respect to *Re*, the Reynolds number can be calculated as shown in Equation (4.6)

$$Re_{turb} = \frac{6.9}{10^{\left(\frac{1}{-1.8\sqrt{f}}\right)} - \left(\frac{\varepsilon/D}{3.7}\right)^{1.11}} \tag{4.6}$$

4.1.4 Viscosity

With both Reynolds number and density known, the apparent viscosity for a given flow rate can be calculated by solving Equation (2.3) with respect to μ_a.

$$\mu_a = \frac{\rho u D}{Re} \tag{4.7}$$

Where ρ, density, is calculated from Equation (4.2) and D is the inner pipe diameter. The average fluid velocity, u is calculated from the flow rate (Equation (2.2)), and *Re* is calculated from Equation (4.6) or (4.7), depending on the fluids flow regime.

4.2 Non-Newtonian fluid

4.2.1 Rabinowitsch Mooney Equation

The Rabinowitsch-Mooney Equation let us calculate viscosity for a non-Newtonian Herschel Bulkley fluid by converting flow rate to shear rate. The following steps will show us how.

The volumetric flow rate through an annular element of area, δQ, perpendicular to the flow and of width δr, perpendicular to the inner pipe radius, R, is given by Equation (4.8) [10]

$$\delta Q = 2\pi R \delta r \cdot u \tag{4.8}$$

The flow rate for the whole pipe is then,

$$Q = 2\pi \int_0^R r u dr \tag{4.9}$$

When integrating this by parts, it gives

$$Q = 2\pi \left\{ \left[\frac{r^2 u}{2} \right]_0^R + \int_0^R \frac{r^2}{2} \left(-\frac{du}{dr} \right) dr \right\} \tag{4.10}$$

Assuming there is no slip at the pipe wall, the first term in Equation (4.10) is neglected, and can be rewritten as

$$Q = \pi \int_0^R r^2 (-\dot{\gamma}) dr \tag{4.11}$$

The shear stress is a function of shear rate only for a time independent and homogeneous fluid [10]. If we inverse this, shear rate is a function of shear stress only, and the variation of τ with r has the following relation:

$$\frac{\tau}{\tau_w} = \frac{r}{R} \tag{4.12}$$

where τ_w is the wall shear stress. With the use of this relation, Equation (4.11) can be written as

$$Q = \pi \int_0^{\tau_w} \frac{\tau^2 R^2}{\tau_w^2}(-\dot{\gamma})\frac{\tau_i}{\tau_w}d\tau = \frac{\tau R^3}{\tau_w^3}\int_0^{\tau_w} \tau^2(-\dot{\gamma})d\tau \tag{4.13}$$

The shear rate, $\dot{\gamma}$, is now a function of τ instead of r. Writing Equation (4.13) in terms of flow characteristics gives [10]

$$\frac{8u}{D} = \frac{4Q}{\pi R^3} = \frac{4}{\tau_w^3}\int_0^{\tau_w} \tau^2(-\dot{\gamma})d\dot{\gamma} \tag{4.14}$$

Where u is the average velocity of the fluid and D is the inner diameter of the pipe. When multiplying Equation (4.14) by τ^3 and differentiating with the right to τ_w it can be rewritten as

$$3\tau_w^2\frac{8u}{D} + \tau_w^3\frac{d(8u/D)}{d\tau_w} = 4\tau_w(-\dot{\gamma})_w \tag{4.15}$$

Solving Equation (4.15) with respect to wall shear rate, $\dot{\gamma}_w$, gives

$$-\dot{\gamma}_w = \frac{8u}{D}\left[\frac{3}{4} + \frac{1}{4}\frac{\tau_w}{(8u/D)}\frac{d(8u/D)}{d\tau_w}\right] \tag{4.16}$$

Rewriting Equation (4.16) based on the relation $dx/x = d\ln x$ gives the Rabinowitsch-Mooney Equation

$$\dot{\gamma}_w = \frac{8u}{D}\left[\frac{3}{4} + \frac{1}{4}\frac{d\ln(8u/D)}{d\ln\tau_w}\right] = \frac{8u}{D}\left[\frac{3}{4} + \frac{1}{4}n_a\right] \tag{4.17}$$

Where

$$n_a = \frac{d\ln(8u/D)}{d\ln\tau_w}$$

The minus sign in front of the shear rate in equation (4.16) is neglected. This is because the absolute values are used for $\dot{\gamma}$ and τ in the calculations above, even though the shear rate for flow in a pipe actually are negative.

4.2.2 Calculation method for flow loop measurements

The required measurements and the calculation method used in the experimental part, based on the Rabinowitsch-Mooney Equation, is presented below.

1. Measure ΔP in the horizontal section for various flow rates.
2. Calculate the shear stress at wall, τ_w $[Pa]$, with equation (4.18)

$$\tau_w(i) = \frac{2RdP_{hor}(i)}{4L} \tag{4.18}$$

3. Establish two vectors

$$x(i) = \ln\left(\frac{8u(i)}{D}\right)$$

$$y(i) = \ln(\tau_w(i))$$

4. Establish the generalized flow index gradient, n_a ($n_a = m$), as a function of x and y for all flow rates and pressure measurements by Equation (4.19)

$$n_a(i) = \frac{y(i+1) - y(i)}{x(i+1) - x(i)} \tag{4.19}$$

5. The shear rate at wall can now be calculated

$$\dot{\gamma}_w(i) = \frac{3n_a(i)+1}{4n_a(i)} \cdot \frac{8u(i)}{D} \tag{4.20}$$

6. Finally, the apparent viscosity (μ_a) as a function of flow rate, Q(i) and pressure measurements are estimated with Equation (4.21)

$$\mu_a(i) = \frac{\tau_w(i)}{\dot{\gamma}_w(i)} \tag{4.21}$$

Where μ_a is given in $[Pa \cdot s]$.

Chapter 5

Experimental work

In this chapter we relate the mathematical models to physical experiments. The physical experiments was mainly done in the drilling hydraulics laboratory by running the flow loop. Part one of the experimental work was done with water in the flow loop and is presented in section 5.1. For section 5.2, the drilling fluids laboratory was used to determine which additives/polymers that should be used in the flow loop study in section 5.3.

5.1 Newtonian fluid

The intention of running the flow loop with water was to calibrate the model. Prior to running the flow loop, the tank was filled with 100 liters of water and the Matlab code and Simulink structure were carefully checked up against theory.

Several days were spent to test the model and evaluate its accuracy. When running the flow loop, some problems came up regarding the pump accuracy. The flow rate went straight up and had a great overshoot before it eventually stabilized at desired flow rate. Even when it stabilized, it still had some error due to a pulse/wavy form. This error was corrected by adding a PID controller in the Simulink structure and calibrating it with K_p, K_i and K_d parameters.

Fig. 5.1. PID values used in this thesis

After adding the PID controller, the pump uses longer time to increase up to desired flow rate, but the overshoot is considerably smaller and the flow rate stabilizes faster. The values shown in Fig. 5.1. above were used for all flow rates, both for Newtonian and non-Newtonian fluid.

To make sure that the flow rate was stable, a sampling interval from 200 to 270 seconds was chosen for every singular flow rate. The sampling rate was set to 0.001, giving 1000 measurements per second. The average dP for each flow rate can be seen in Appendix C. When running the Matlab™-code after sampling the dP data for each flow rate, the average value for the 70 second sampling window were automatically calculated and the value was typed into an Excel sheet (Appendix C). The following figure illustrates the stability for a 45 l/min flow rate during the 70 second window.

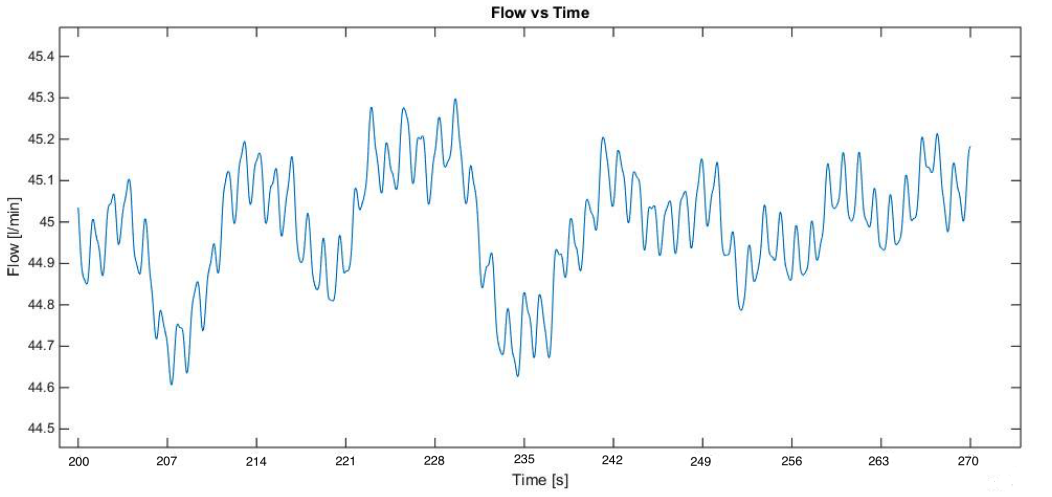

Fig. 5.2. Flow rate vs Time

As seen, there are still some inaccuracy/pulses for the flow rate, but it's as close as it could get for this setup.

The corresponding horizontal- and- vertical dP are shown in Fig. 5.3. and 5.4.

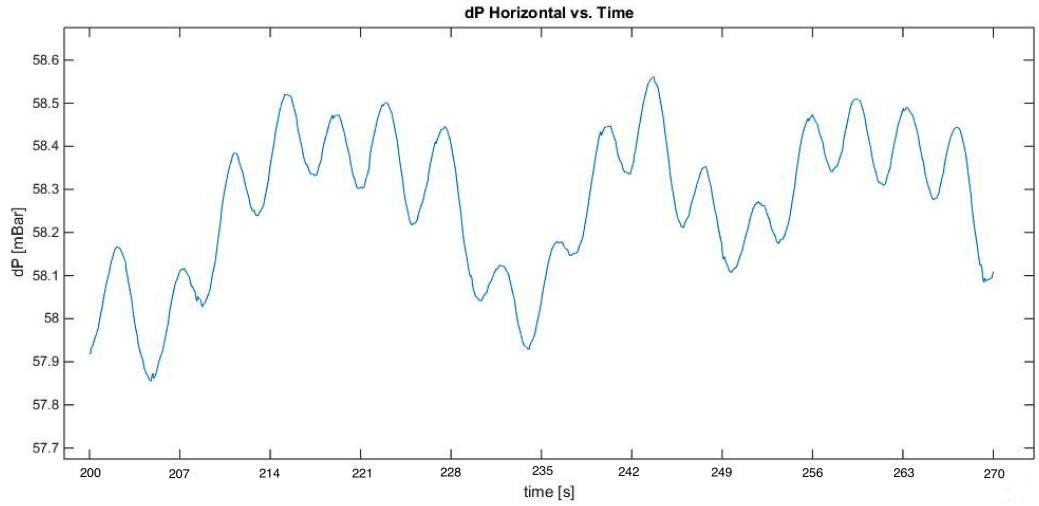

Fig. 5.3. Horizontal dP vs time

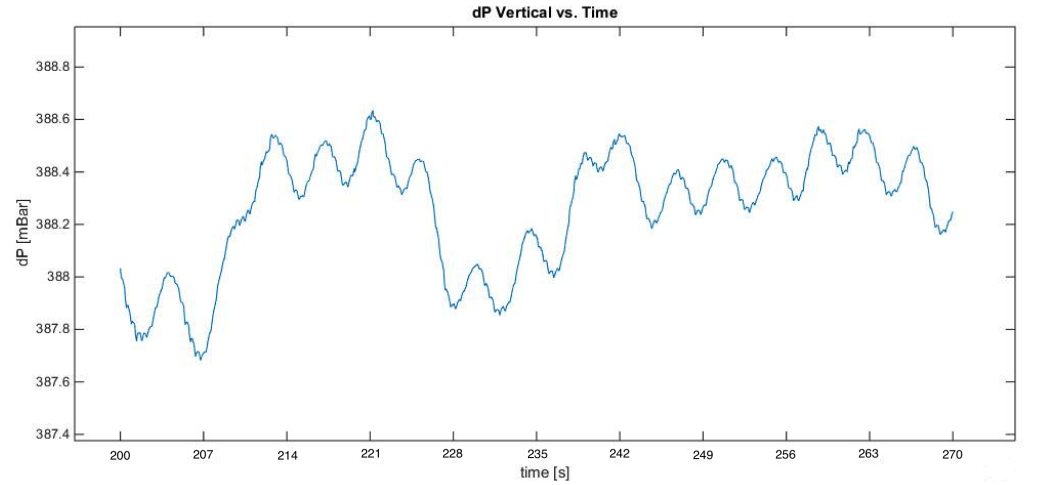

Fig. 5.4. Vertical dP vs Time

5.1.1 Water Density

Combining the data laying behind the figures above with Equation (4.3), the density is estimated and shown in Fig. 5.5.

As seen from the figure, water density is lower than its theoretical value (1000 kg/m^3) as a result of some inaccuracy with the dP sensors. In total it was taken 32 measurements like the one above for flow rates from 90 to 10 liter/min. This is the largest interval that the pump could deliver for water, and still stay stable. All measurements are listed in Appendix C.

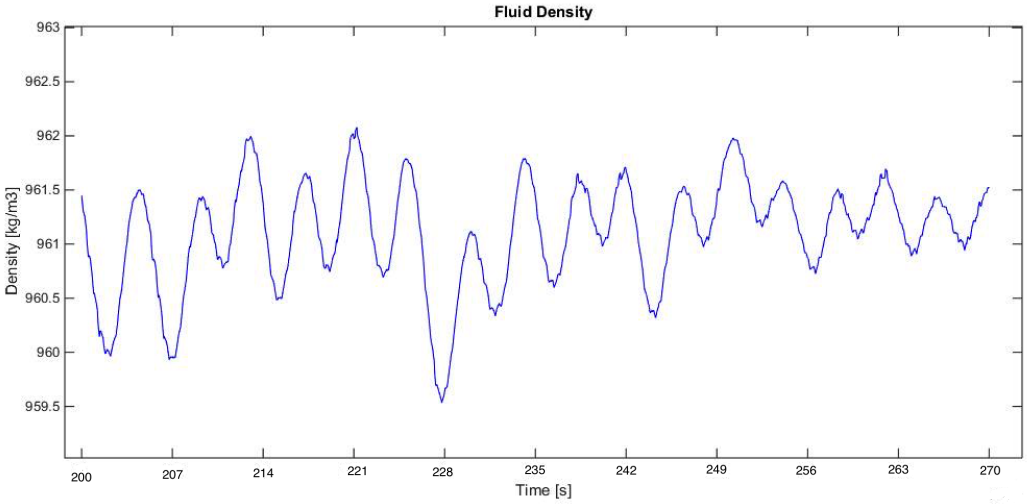

Fig. 5.5. Density vs Time

When plotting all measurements for vertical and horizontal dP, the following figure illustrates how the (relative pressure drop) changes when we subtract the horizontal dP from the vertical, as we decrease the flow rate step by step from 90 l/min to 10 l/min.

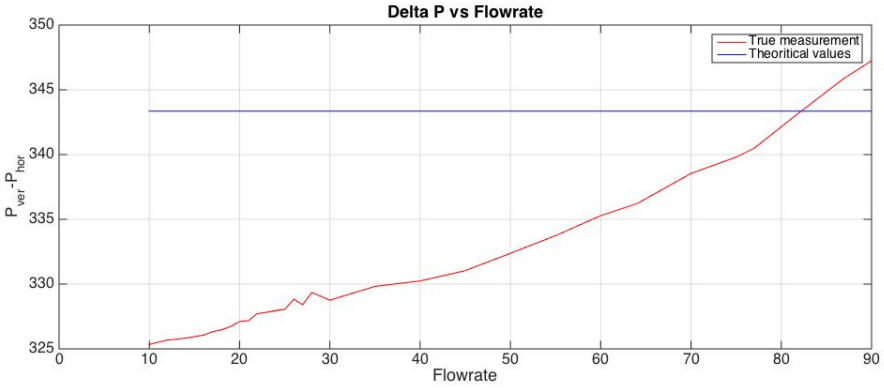

Fig. 5.6. dP vs Flow rate

The theoretical dP value for water should be a horizontal line for all flow rates, and is illustrated with a blue line in Fig. 5.6. The theoretical value is equal to the hydrostatic pressure of the fluid, which is used to calculate the density. Combining the measured ΔP with Equation (4.3) gives us the following values for the water density.

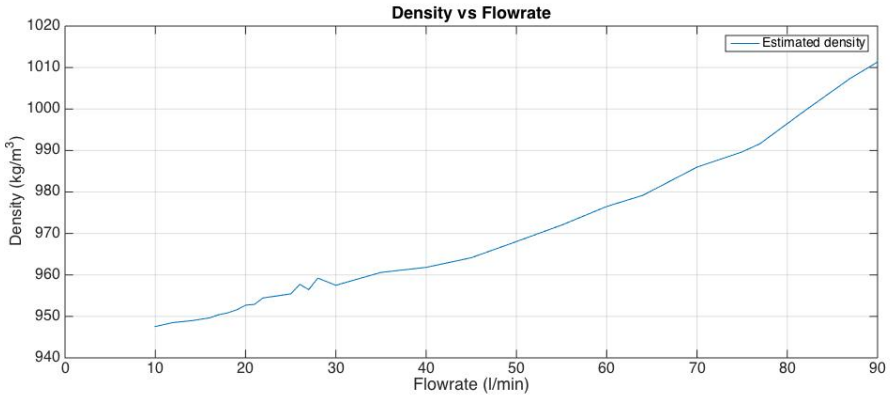

Fig. 5.7. Density vs Flow rate

As seen from Fig. 5.7, density changes with flow rate as a result of non-constant dP. This can be explained by a systematic error, as the sensors tend to drift for different flow rates. To make up for the dP error, it was necessary to introduce an offset formula based on the gap between the theoretical and estimated value. The offset in [mBar] for each flow rate is expressed in Fig. 5.8. A regression model based on the offset data is made in Matlab and included in the figure.

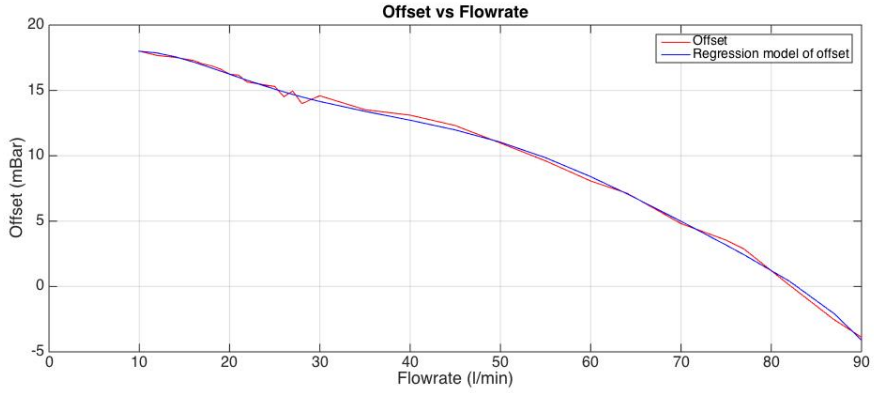

Fig. 5.8. Offset (mBar) vs Flow rate

The regression model was created with the *polyfit* function in Matlab™, which is presented in Appendix A (Fig. A.1.). When including the offset model to the ΔP measurements, the water density was again calculated and shown in the following figure.

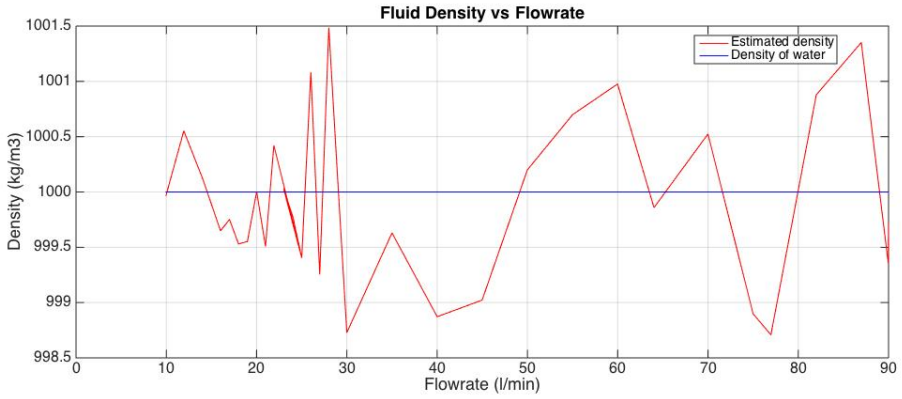

Fig. 5.9. Fluid density vs Flow rate

After the offset correction was added to the dP measurements the density variates with $+/-$ 0.15 % (1.5 kg/m^3) which gives an accuracy of 99.85 %. This was assumed acceptable. By adding a low pass filter to the new estimated density, the result will be improved again as it blocks out the highest frequencies. Fig. 5.10. compares the density after low pass filter was added (red line), with unfiltered density and the theoretical value for water. The size of the filter-window was set to 10 on the x-axis, filtering out the highest frequencies for every 10 l/min.

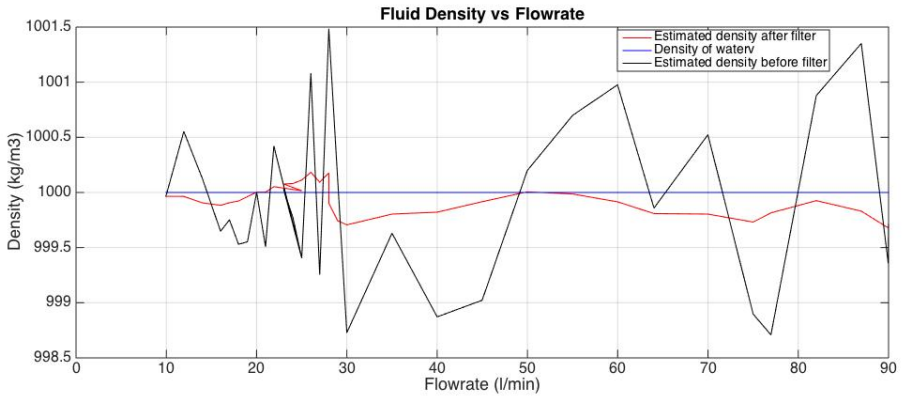

Fig. 5.10. Density after filter vs Flow rate

The estimated density after low pass filter was added variates with 0.03 % at most, which gives an accuracy of 99.97 %. The density calibration are giving satisfying results.

5.1.2 Viscosity

To be able to calculate the viscosity of water using the flow loop, Darcy-Weisbach friction factor needs to be estimated, using Equation (4.4). Further, the Reynolds number had to be determined, until the viscosity finally could be calculated.

Fig. 5.11. shows the Darcy friction factor for every flow rate tested between 10 and 90 l/min.

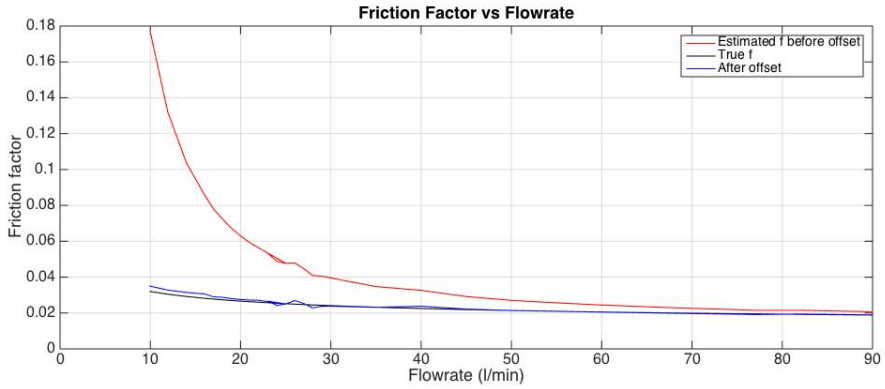

Fig. 5.11. Darcy-Weisbach friction factor vs Flow rate

The red lines represents the friction factor without offset correction, while the blue line is after a constant offset correction of 14 *mBar* has been added to the horizontal differential pressure. The offset correction seems to be giving a value really close to the theoretical.

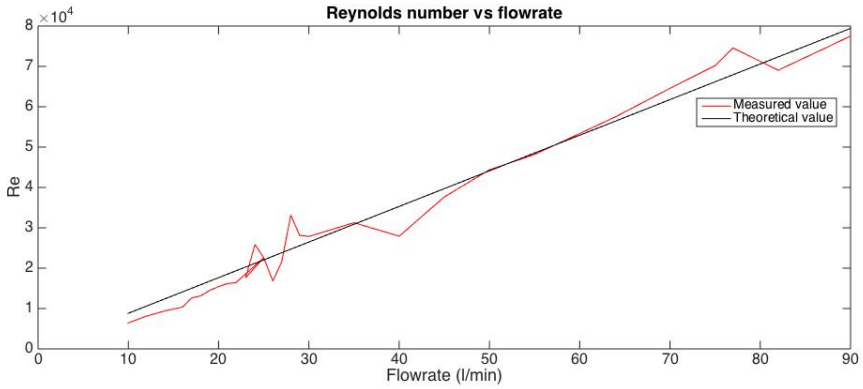

Fig. 5.12. Reynolds number vs Flow rate

From Fig. 5.12. we can read a measured Reynolds number of approximately 8700, which indicates turbulent flow. Equation (4.6) was therefore used to calculate the Reynolds number for all flow rates. The friction factor used in Equation (4.6) is the offset corrected Darcy-Weisbach friction factor.

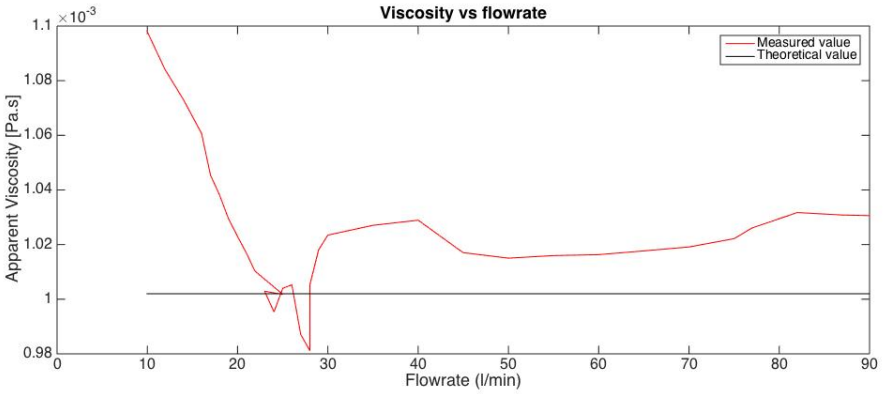

Fig. 5.13. Apparent Viscosity vs Flow rate

The offset correction gave an apparent viscosity, μ_a, close to 1 cP (Fig. 5.13.), which is the theoretical value for water in room temperature (20 °C). The model looks promising with the current modifications and the same offset correction will be further tested when adding polymers to the water in section 5.2.

5.2 Non-Newtonian fluid

Before Xanthan gum was chosen as the additive that would be tested in this thesis, the possibility of using different types of fluid was investigated. Bentonite is one of the particles that was mentioned in several thesis's when discussing further research in the drilling hydraulics laboratory. After discussing the possibilities of using bentonite drilling fluid in the flow loop with the person responsible for the drilling hydraulics laboratory, the conclusion was that it was not recommended, and the only way to clean the flow loop afterwards was to disassemble the entire rig. The best alternative to run the flow loop with a non-Newtonian fluid was to use a polymer that would not damage the pump or leave traces in the pipe joints.

The options for additives to a non-Newtonian fluid was then narrowed down to polymers like PAC (Polyanionic Cellulose) and Xanthan gum, which both increase the viscosity in water. When looking at samples from the two mixtures, PAC looked like the best option as bubbles were less dispersed in the fluid, and because Xanthan gum would start to rot after three to four days when mixed with water. However, the University had only half a kilo PAC in stock, and unfortunately no more PAC could be bought at this time, after trying to contact several suppliers.

Since the flow loop requires a great amount of fluid in the tank to run the system, two types of Xanthan gum was further tested, as these polymers are easier to get hold of. The two are named Xanvis and Duotech NS. Because of the rotting process of Xanthan gum, it was

of great interest to choose the most stable Xanthan gum when it comes to viscosity, since mixing of that amount of fluid and all the tests to be done in the flow loop, couldn't be done in one day.

5.2.1 Testing of Xanvis and Duotech NS

Several samples of the two polymers were mixed and tested over a period of 3 days to evaluate the viscosity and durability of the fluid.

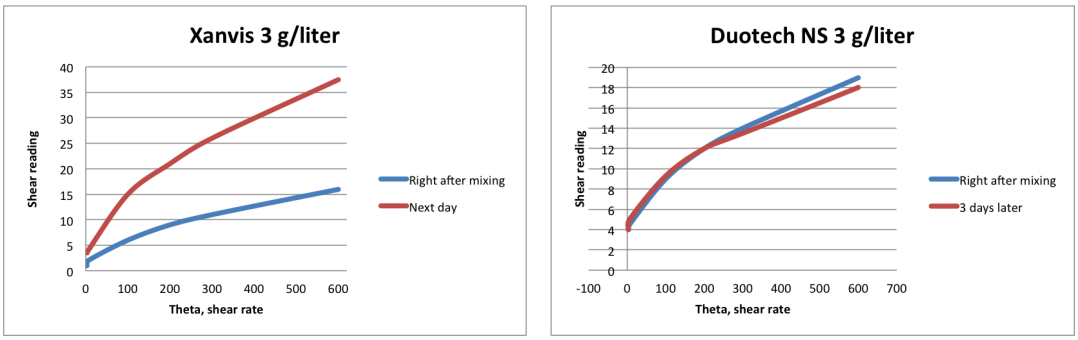

(a) Rheology Xanvis 3 g/liter **(b)** Rheology Duotech NS 3 g/liter

Fig. 5.14. Rheology 3 g/liter

Fig. 5.14. shows the measured shear readings at different times for the two fluids, by using a Fann®35 viscometer. As seen from the figures, the Duotech NS samples seems to be much more stable compared with Xanvis.

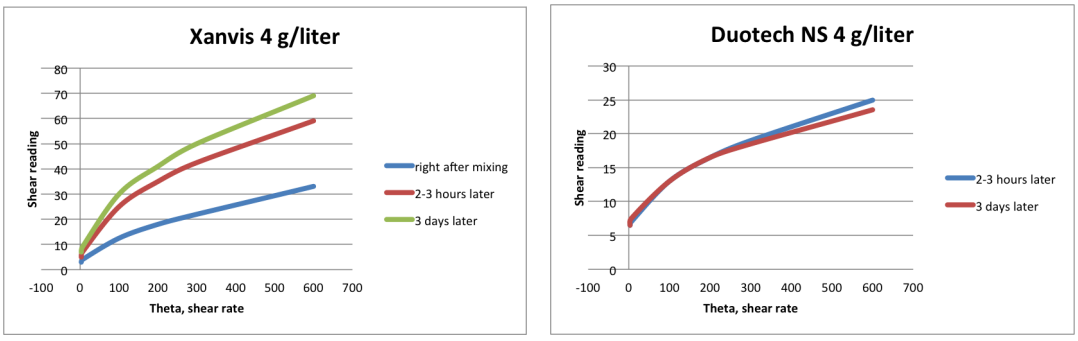

(a) Rheology Xanvis 4 g/liter **(b)** Rheology Duotech NS 4 g/liter

Fig. 5.15. Rheology 4 g/liter

The same trend can be seen in Fig. 5.15. Xanvis has higher shear readings than Duotech NS, but Duotech doesn't change that drastic over time. Another thing that was observed during mixing of these batches was that the Duotech fluid generated some bubbles due to

high rotational speed on the propeller with the Hamilton Beach Mixer. Since the large fluid mixer in the drilling fluid laboratory (that would be used to mix up the batches for the flow loop) can be set to a much lower rotational velocity, this was not seen as a problem for the flow loop experiment. The final decision was to use Duotech NS.

Two bachelor students decided to use Duotech NS as well for their experiments. The laboratory at UiS had only one kilo available at the time, but we were provided a 25 kg sack of Duotech NS from Hydrawell. Everything was finally in place to begin the flow loop experiments with non-Newtonian fluid.

5.2.2 Preparing the Xanthan gum fluid

For the experimental study it was decided to use three different concentrations of Duotech NS, 3 g/liter, 4 g/liter and 5 g/liter. The results from the flow loop will be calculated from the Rabinowitsch-Mooney Equation based on the flow rate and pressure drop, and will be compared with density and calculated apparent viscosity from the mud balance scale and the Fann®35 viscometer.

The fluid was mixed 15 liters at a time in a large bucket, using the Ystral X 50/10 fluid mixer. When mixing the first batch of 3 g/liter, 45 grams of Duotech NS was gently mixed into 15 liters of water over a 5 to 10 minutes period, before the batch was left with the mixer on for an additional 25 minutes. Problems regarding bubbles in the fluid with the Hamilton Beach mixer was also eliminated with the Ystral mixer due to lower rotational speed. There was close to zero visible bubbles in the fluid after the batch was ready-made.

Fig. 5.16. Ystral mixer

The fluid was then carried down to the drilling hydraulics laboratory and poured over in the tank. This procedure was repeated 6 times for each batch until the tank was filled with 90 liters of fluid. After the tank was filled with Duotech NS fluid in the afternoon, it was left to settle until the next day. Each batch made followed the same procedure regarding mixing and settling time.

5.3 Flow loop study with non-Newtonian fluid

Before starting up the flow loop, a sample was taken from the tank and brought to the drilling fluid laboratory. Density was then measured with a mud balance scale and the Fann®35 was used to measure the shear stress.

The flow loop was then turned on remotely from Simulink with a maximum flow rate which happened to be 87 l/min for the 3 g/liter Duotech NS fluid. It took around 120 seconds from the start button was pushed until the given flow rate had stabilized. Sample time was therefore set in Matlab™, from 140 to 180 seconds to ensure accurate measurements.

5.3.1 Density measurement - Duotech NS 3 g/liter

The density calculation procedure is the same for non-Newtonian as for Newtonian fluid, where $dP_{ver} - dP_{hor}$ are measured and plotted with Equation (4.3) against flow rate.

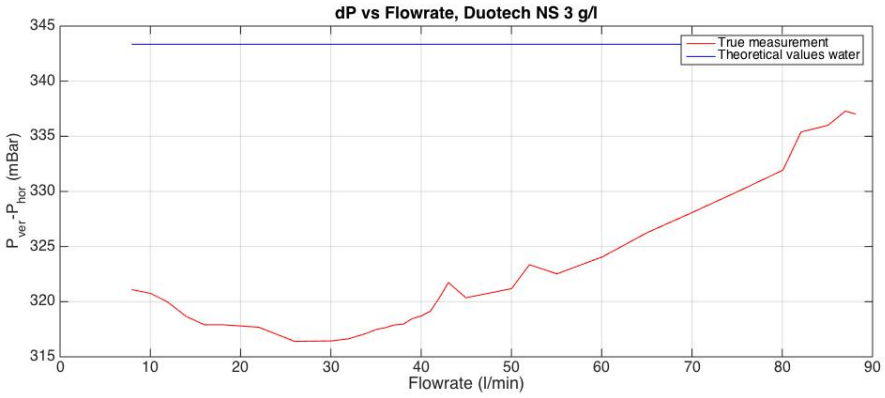

Fig. 5.17. dP for Duotech NS - 3 g/liter

Fig. 5.17. illustrates the differential pressure for all flow rates measured in the experiment. It is compared with the theoretical value for water, where the differential pressure corresponds to a fluid density of 1000 kg/m^3. The calculated density based on dP for Duotech NS above is illustrated in Fig. 5.18. This density includes the same offset correction used for water in section 5.1.

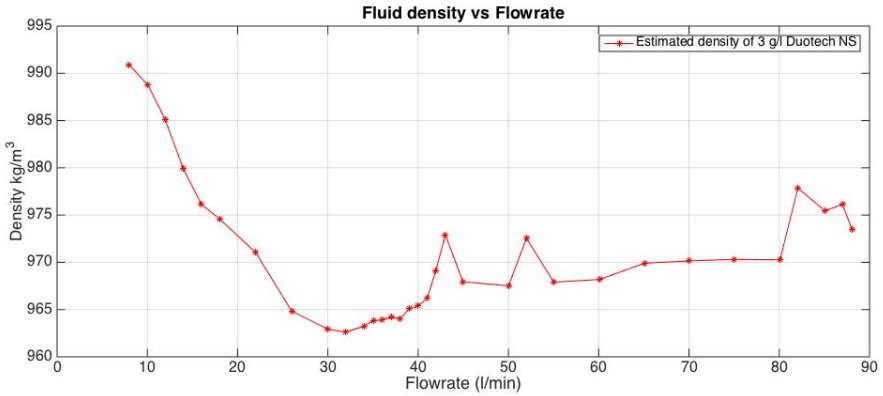

Fig. 5.18. Estimated Density - Duotech NS 3 g/liter

The actual measured density of the sample taken from the tank before starting the flow loop was close to 0.995 SG, which happened to be the case for every batch when using a simple mud balance scale. When using a pressurized mud balance scale, the density got the same value as water, 1.00 SG, since the amount of additive is relatively small compared with the 90 liters of water.

As we can see from Fig. 5.18, the measured density, including offset correction, is off with around 30 kg/m^3 for most flow rates when we go from high to low flow rates. The density does however increase from 30 liters/min as we decrease the flow rate step by step all the way down to 8 liters/ min.

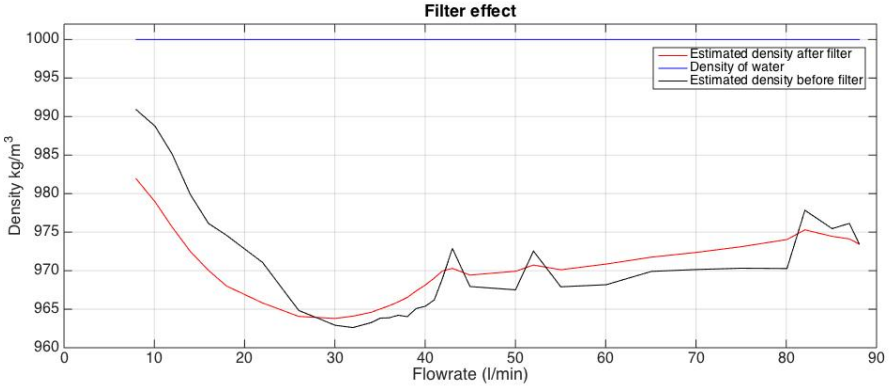

Fig. 5.19. Estimated Density before and after low pass filter

Fig. 5.19. shows that the low pass filter cuts out the largest spikes, thus giving an average density for all the flow rates. The filtering window size for the Duotech fluid is the same as for water, 10 on the X-axis. For lower flow rates there is a larger gap between the estimated density and the filtered density (between 10 to 15 kg/m^3) because of the steep increase in measured density.

There are probably several reasons to explain the low density, compared with the theoretical value measured in the laboratory. This will be further discussed in chapter 6. However, it is reasonable to state that the biggest reason is due to air bubbles that are generated in the fluid when running the flow loop.

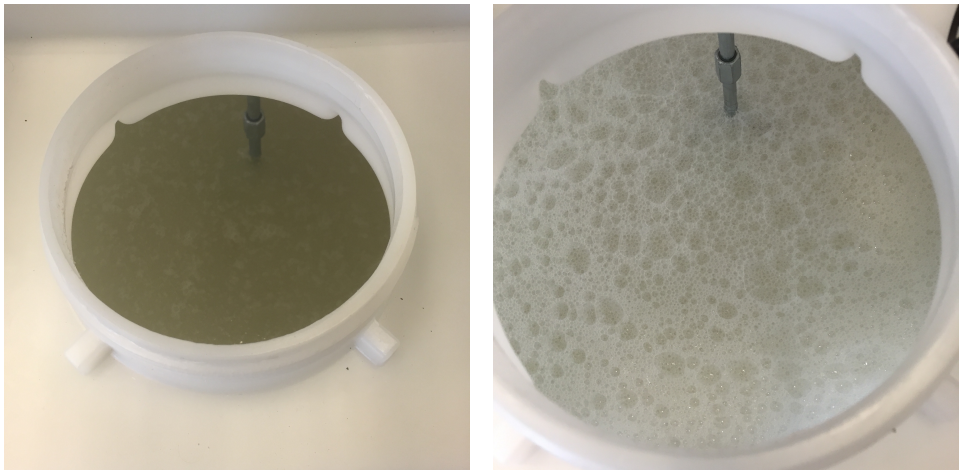

(a) Before running the flow loop **(b)** After running the flow loop

Fig. 5.20. Foam generation

In Fig. 5.20 b), a foam layer is laying on top of the fluid. The layer kept increasing up to somewhere between 12-18 cm as the flow loop continued to run through all the flow rates. From Fig. 5.21 b) the bubbles are clearly seen in the pipes when turning of the flow loop.

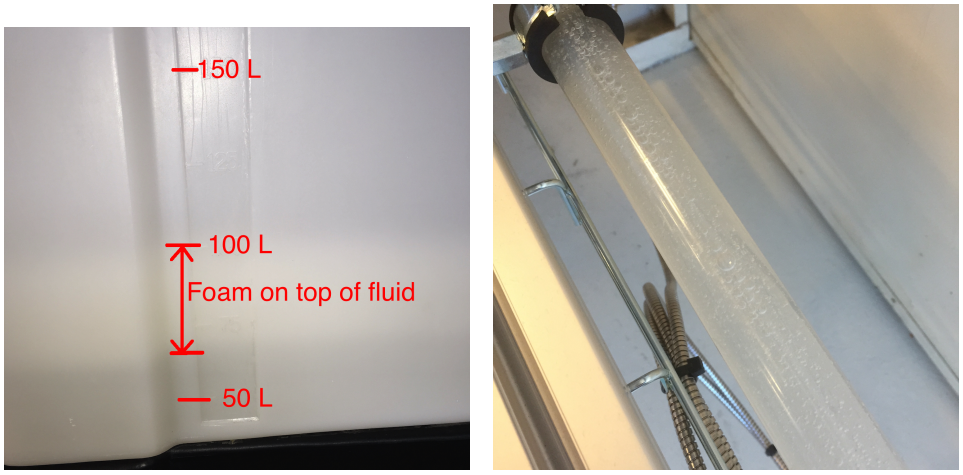

(a) Foam layer on top of fluid **(b)** Bubbles in the fluid after shutdown

Fig. 5.21. Foam layer in tank and bubbles in fluid

5.3.2 Density measurement - Duotech NS 5 g/liter

The next batch made was a 5 g/liter concentration. The same procedure was followed for mixing the fluid and the settling time. A sample was taken from the tank to test rheology and density properties of the fluid in the drilling fluid laboratory before running the flow loop. As mentioned earlier, the density was some place close to 0.995 SG for the sample fluid.

After running the flow loop for flow rates ranging from 10 to 87 l/min, the differential pressure was plotted based on the Matlab™-code seen in Appendix A (Fig. A.2).

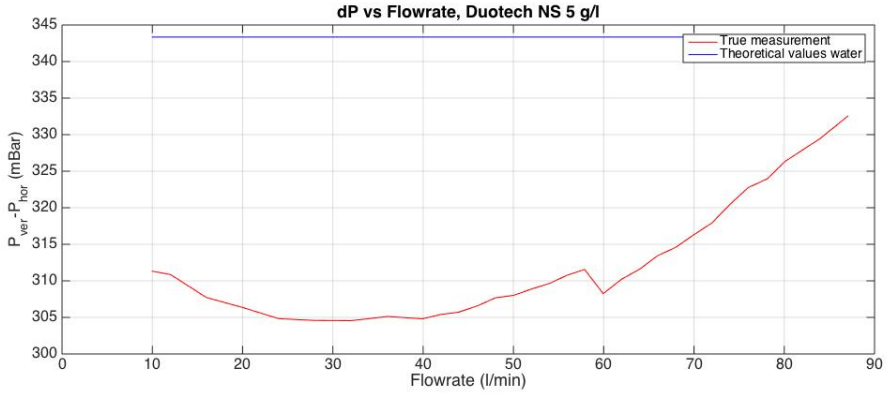

Fig. 5.22. dP for Duotech NS - 5 g/liter

Fig. 5.22 illustrates a lower differential pressure compared with the first batch, 3 g/liter. Higher concentrations of Duotech NS in the water will make the fluid more viscous, but also result in even more bubbles when running the flow loop.

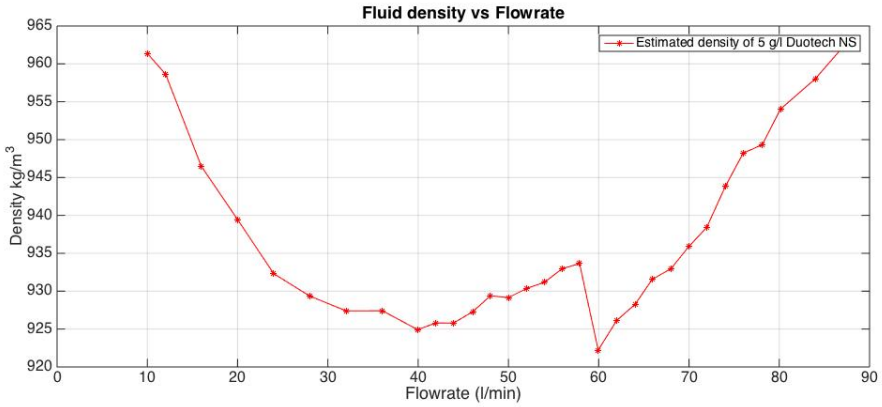

Fig. 5.23. Estimated Density - Duotech NS 5 g/liter

The density seen in Fig. 5.23 confirms what was mentioned regarding more bubbles in the fluid as the density drops an additional 30 kg/m^3 at the lowest, compared with the first

batch. It is also to be seen that the density has a steeper drop in Fig. 5.23. when starting the flow loop at 87 l/min, compared with the 3 g/liter density plot (Fig. 5.18). The most logical reason for this is that the flow loop was run several times without sampling the data for the first batch, in order to figure out how long time it takes before the flow rate stabilizes. A lot of bubbles were therefore already created when the first measurements were done for the 3 g/liter fluid. The result of this is a lower density from start and a less steep curve when starting the measurements, compared with Fig. 5.23, where the 5 g/liter fluid was measured from the first time the pump was turned on.

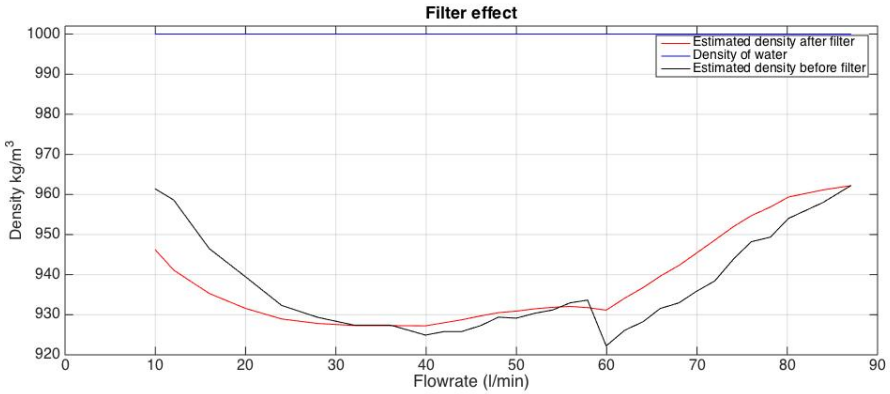

Fig. 5.24. Estimated Density before and after low pass filter

Again, the low pass filter makes a smoother and a less steep slope as the density decreases with increased amount of bubbles in the fluid. The window size for the low pass filter is the same as for the previous batch.

5.3.3 Density measurement - Duotech NS 4 g/liter

Due to the accumulation of bubbles in the fluid when running the flow loop, the testing procedure was changed for the last batch. The mixing procedure was the same for 4 g/liter as for the two previous batches, but this time, a total of 6 density tests and 5 rheology tests were done in the laboratory while running the flow loop for different flow rates. Prior to starting the measurements, the pump circulated the fluid for 10 minutes, to see if the steep slope seen from 90 to 60 liter/min in Fig. 5.23 would disappear

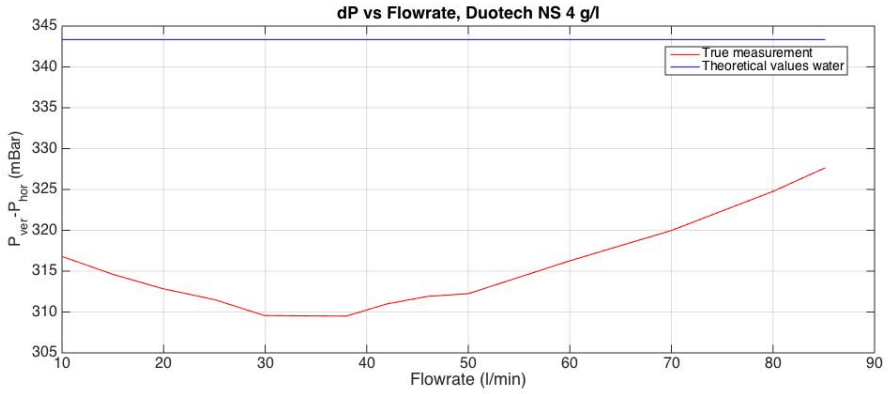

Fig. 5.25. dP for Duotech NS - 4 g/liter

It can be seen from Fig. 5.25 that the dP curve is less steep for the 4 g/liter batch, compared with the 5 g/liter, as foreseen. The dP values are closer to the 5 g/liter values than the 3 g/liter curve, but the pressure sensors proved to measure the dP in right order.

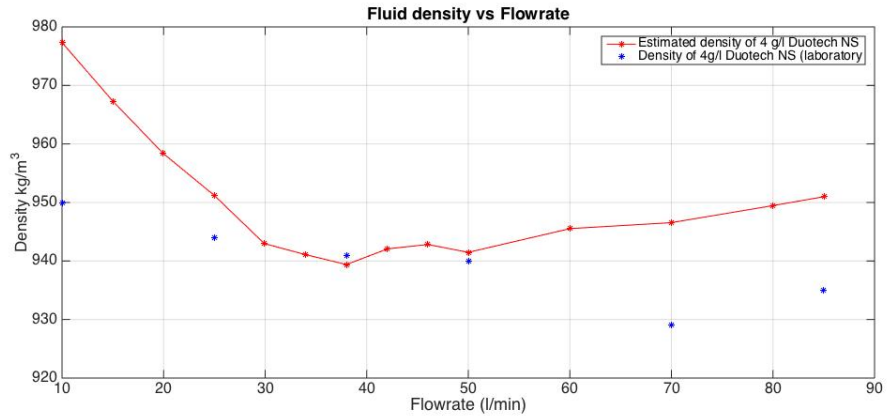

Fig. 5.26. Estimated Density - Duotech NS 4 g/liter

The estimated density from the pressure measurements is compared with the density measurements done in the laboratory for certain flow rates, as it was decreased step by step. The red line represents the estimated density for all flow rates that was used in this experiment, while the blue dots are the actual measured density from samples taken from the tank. These measurements can be seen in Table 5.1.

From Fig. 5.26 it can clearly be seen that the slope of the density curve is significantly less declined in the beginning, since the flow loop had already generated bubbles in the fluid before starting the measurements. It is also worth mentioning that the first two measurements done in the laboratory seems a little off compared with the rest. This could be explained by a thin foam layer on top of the fluid, seen in Fig. 5.20 a). For the last four measurements the

Table 5.1. Density measurements in laboratory

Flow rate (l/min)	Density (kg/m^3)
85	935
70	929
50	940
38	941
25	944
10	950

thin foam layer was gently wiped off and the laboratory density seems to fit the estimated density curve better from 50 to 25 liter/min. Fig. 5.27 b) compares the density measurement done after running the flow loop with a flow rate of 70 l/min with the measurement done after running the flow loop with a flow rate of 38 l/min (Fig. 5.27 a). The amount of foam on top of the fluid in figure b) can explain a lower density relative to the measured value from the flow loop, seen in Fig. 5.26.

(a) Bubbly fluid **(b)** Bubbly fluid with foam

Fig. 5.27. Bubbly fluid in mud balance scale cup

Fig. 5.28 illustrates the filter effect on density. The filtered density slope seems to be close to 950 kg/m^3 which is near the measured values done in the laboratory.

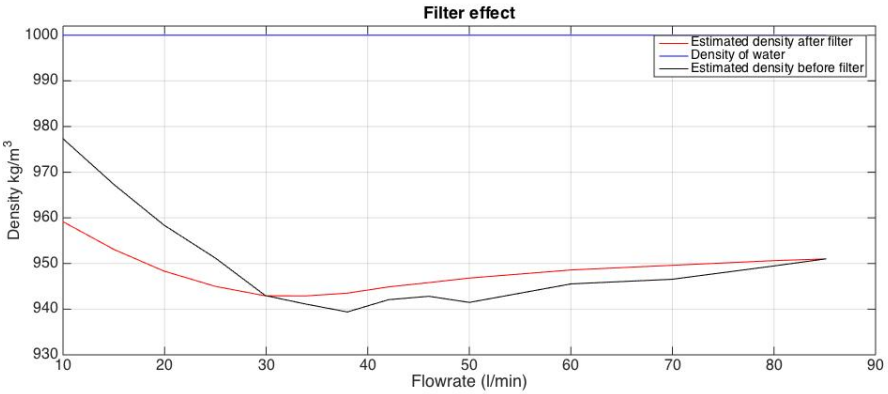

Fig. 5.28. Estimated Density before and after low pass filter

5.3.4 Viscosity estimation

Based on the Rabinowitsch-Mooney Equation (Equation (4.17)), apparent viscosity was calculated by the procedure in section 4.2.2. Differential pressure measurements in the horizontal section was used to estimate the shear stress at wall, τ_w, for all flow rates. When τ_w and the average fluid velocity is known, the generalized flow index gradient, n_a, could be estimated based on Equation (4.19). Further, the n_a-gradient was used in the calculation of the shear rate at wall (Equation (4.20)). Finally the apparent viscosity for the 3 g/ liter batch was estimated and can be seen in Fig. 5.29.

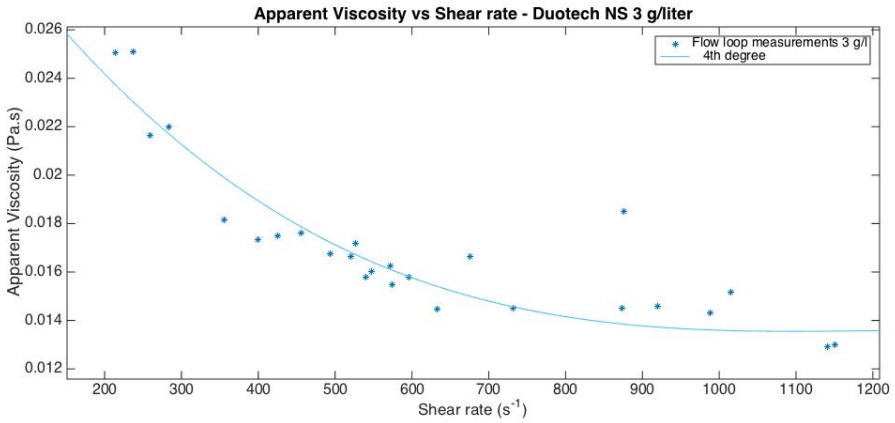

Fig. 5.29. Apparent viscosity ($Pa \cdot s$) for 3 g/liter batch

The apparent viscosity is increasing from 13 to 25 cP when decreasing the flow rate from 87 to 8 liter/ min. A trend line was added to the plot by using the basic fitting tool in Matlab™. The viscosity measurements had the best fit with a 4th degree polynomial formula from fitting tool-box. The lowest shear rates in the plot is close to 200 s^{-1}, which is a result

of a minimum flow rate of 8 liters/min. If the pump could provide stable flow for lower flow rates, more viscosity data would be added to the plot.

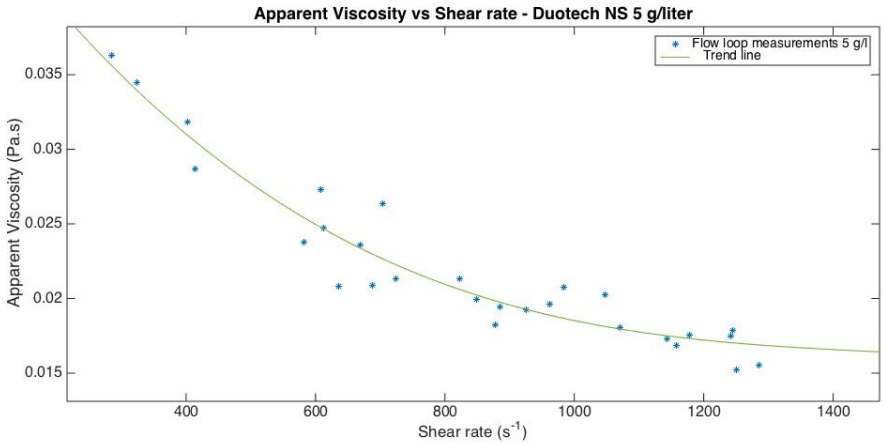

Fig. 5.30. Apparent viscosity ($Pa \cdot s$) for 5 g/liter batch

Fig. 5.30 illustrates the apparent viscosity for the 5 g/liter batch for flow rates between 87 and 10 l/min. The estimated values has the same trend as Fig. 5.29, where the lowest shear rates lay around 200 to 300 s^{-1} for the Duotech 5g/liter fluid. The corresponding viscosity values are stretching from 15 cP and all the way up to 35 cP. The ability to flow is therefore almost the same as for the 3 g/liter batch for high shear rates, while for lower shear rates, the resistance to flow is greater.

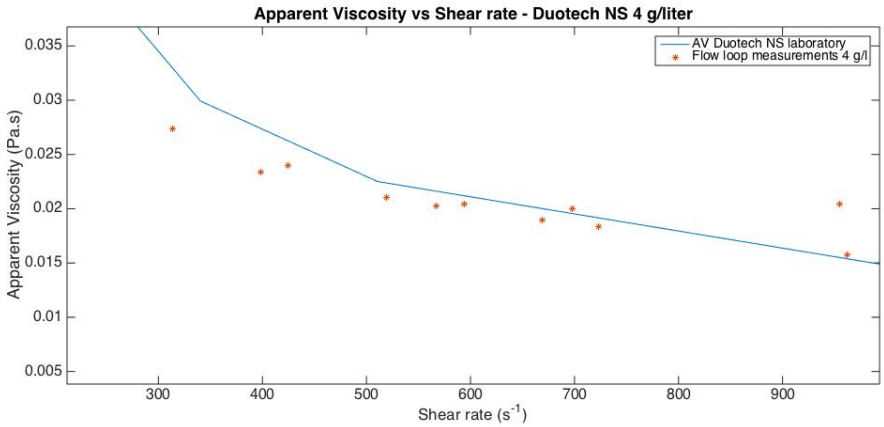

Fig. 5.31. Apparent viscosity ($Pa \cdot s$) for 4 g/liter batch

In Fig. 5.31, the estimated apparent viscosity (AV) from the flow loop is compared with AV calculated from the Fann®35 readings for the 4 g/liter batch. The lowest viscosity value is close to 15 cP, while the highest estimated AV value is 27 cP for a shear rate around 300 s^{-1}. From Fig. 5.31. it is possible to see that the calculated AV from the Fann ®35 measurements are a little higher for low shear rates, compared with the estimated AV from the flow loop.

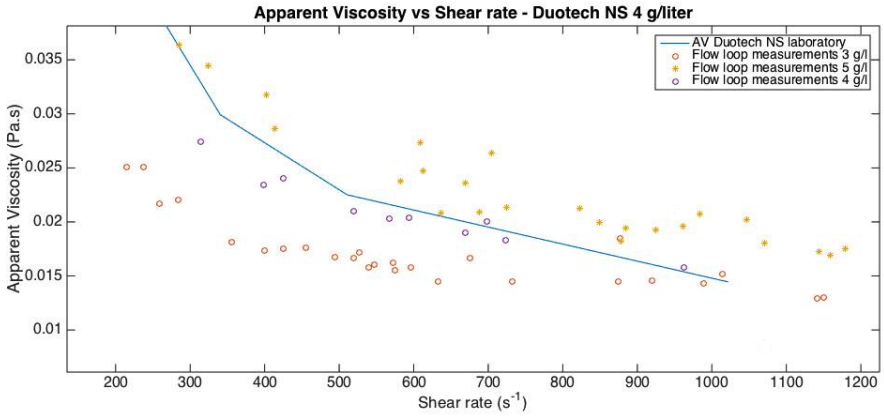

Fig. 5.32. Apparent viscosity ($Pa \cdot s$) for all batches

Fig. 5.32. compares all three batches against each other. The calculated AV from the drilling fluid laboratory for the 4 g/liter batch is also added to the plot.

5.3.5 Back-calculation of drilling laboratory samples

In this section the measured horizontal frictional pressure drop, dP_{hor}, is compared with the estimated horizontal frictional pressure drop based on the calculation method presented in section 2.5.2. The parameters, K, n and τ_y are estimated from the shear readings in Table 5.2.

Table 5.2. Duotech NS - Shear readings from laboratory

RPM	Shear readings 4 g/l
600	28.0
300	23.0
200	20.8
100	17.0
6	10.5
3	9.5

n was calculated with the above mentioned shear readings with Equation (2.7), and further the generalized Herschel Bulckley Reynolds number, Re_{HB-gen}, was estimated with Equation

(2.13). The effective diameter during transient phase and turbulent flow was calculated with Equation (2.15). Following, the modified form of the Haaland's equation (Equation (2.16)) was used to the estimate the friction factor during the transient phase and turbulent flow regime, while for laminar flow, the friction factor was estimated with a modified version of Equation (2.4):

$$f = \frac{64}{Re_{HB-gen}} \tag{5.1}$$

The measured frictional/horizontal pressure drop with the flow loop is compared to the pressure drop estimated from Equation (2.17) in figure 5.33. The Matlab™-code is presented in Appendix A (Fig. A.4)

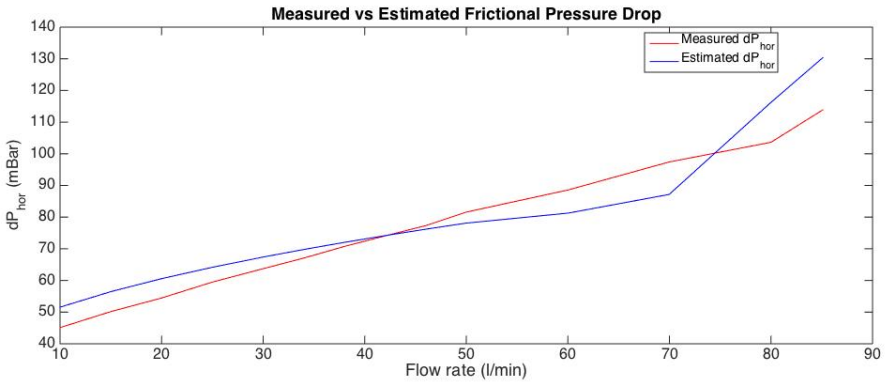

Fig. 5.33. Measured vs estimated frictional pressure drop

Fig. 5.33. illustrates a decent relationship between the measured and estimated frictional pressure drop in the horizontal section for the 4 g/liter batch, especially for flow rates under 50 l/min. A small dip in dP_{hor} for the blue line around 50 liter/min can be observed, and most likely be explained by the change from laminar to transient phased flow regime. For flow rates above 70 l/min, the flow regime changes again to a turbulent flow.

For the measured frictional pressure drop, there is no clear sign of the transition between laminar and transient flow regime, thus, something seems to happen around 50 and 80 l/min. This might be the two transitions between laminar-transient and transient-turbulent.

The largest difference between the measured pressure drop and the estimated are for flow rates between 60 and 70 l/min. This will be further discussed in chapter 6.

Apparent Viscosity back calculation

Based on the generalized Reynolds number and the effective inner diameter of the pipe, the apparent viscosity can be back calculated from the measured flow rates with Equation (2.18). In Fig. 5.34. this procedure is compared with the estimated apparent viscosity from the Fann®35 readings. The back calculation procedure gives lower AV values compared with the estimated AV values in Fig. 5.31, that were calculated with Equation (4.21), based on the Rabinowitsch-Mooney equation.

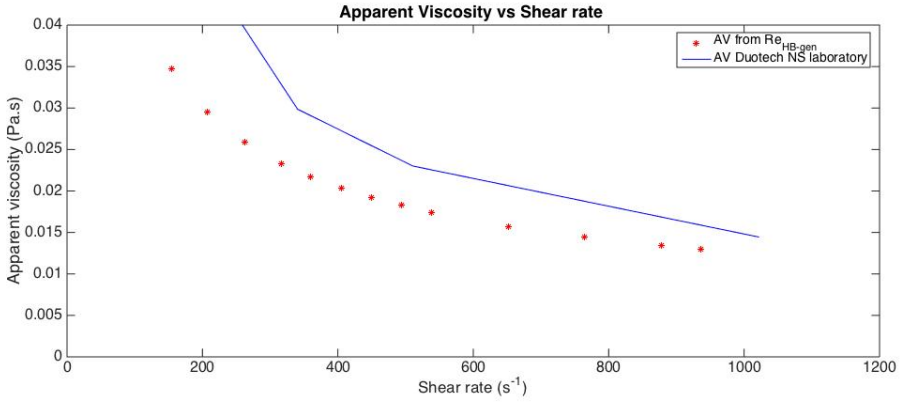

Fig. 5.34. Apparent Viscosity vs Shear rate - Back calculation

Chapter 6

Discussion

6.1 Newtonian fluid

The results for Newtonian fluid in chapter 5.1 are discussed in this section.

6.1.1 Water density

Based on Fig. 5.6. it is reasonable to say that the pressure sensors are having some trouble measuring the accurate differential pressure when water is pumped through the pump. This leads to an estimated density that vary from 1011.7 kg/m^3 for an average flow rate of 89.99 l/min, down to a density of 947.5 kg/m^3 for a flow rate of 9.96 l/min, seen in Fig. 5.7. Some error were expected, but there could be ways to minimize the interval between theoretical differential pressure and the measured values. With the current setup there is a small gap between the pressure sensors and the flow [6]. If the pressure sensor were installed closer to the actual flow, measurements could be improved.

However, in this thesis we introduced an offset correction based on the regression line in Fig. 5.8. When adding the offset correction to the ΔP values, the estimated density came really close to the theoretical value. After filtering out the noise with a low pass filter, the density estimation got even better and the model looked promising as viscosity calculation was next in line.

6.1.2 Viscosity

When the offset correction for pressure drop is included in the calculation of friction factor (Equation (4.4)), the result is almost identical to the theoretical value for flow rates above 25 liter/min. As the flow rate is decreased from 30 to 10 l/min there is an small increase in

the estimated friction factor compared with the theoretical, but this was considered to be reasonable.

The Reynolds number in Fig. 5.12. seems to be following the theoretical value, with small variations for certain flow rates. These variations are expected as the Reynolds number is dependent on the friction factor, and where we see a difference in friction factor, there will also be a difference between estimated and theoretical Reynolds number.

With both Darcy-Weisbach friction factor and Reynolds number close to their theoretical values, the apparent viscosity was estimated to be really close to the real apparent viscosity for water in room temperature (1 cP).

To sum up, the model gives both density and apparent viscosity values close to theoretical values for water, after correcting for the differential pressure offset.

6.2 Non-Newtonian fluid - Duotech NS fluid

The results from running the flow loop with non-Newtonian fluid, presented in section 5.3, are discussed in this section.

6.2.1 Density

During the preparation of the first Xanthan gum (Duotech NS) fluid it looked really promising, as the fluid was viscous with no bubbles. If the fluid had stayed like this when running the flow loop, a density close to the water density would be expected when adding the offset regression model found in section 5.1.1. However, a far lower fluid density was observed due to all the generated bubbles when running the flow loop.

The pressure drop keeps decreasing when going from high flow rates down to 40 l/min for all fluid batches. It is therefore reasonable to say that for flow rates in this interval, an increasing number of bubbles is generated. When the flow rate drops below 30 l/min there is an increase in differential pressure drop. The fluid is in a laminar condition and the increased pressure drop is most likely because of a settling reaction, as no additional bubbles are generated for these flow rates.

A more reasonable result was obtained for the 4 g/liter batch when the laboratory tests were done simultaneously. This procedure is therefore recommended for students that will use the flow loop in the future. From Fig. 5.26 there is a great relationship between the estimated density with the flow loop and the measured density from the laboratory for flow rates between 25 and 50 l/min. With the mud balance scale there is always a risk of human errors, such as the level bubble might not be 100% in center, or the fluid could have some

foam on top of it as in Fig. 5.27 b). However, the laboratory measurement proves that the pressure drop sensors can measure a pressure drop close to the theoretical values when adding the offset correction for water.

6.2.2 Viscosity

From the viscosity plots we can see a great trend, where the apparent viscosity increases for higher concentrations of additives. Fig. 5.32. illustrates how the AV changes with shear rate. For high shear rates, the measured viscosity is closer to each other than for low shear rates. This behavior are expected for shear thinning fluids.

The figure also indicates a good relationship between the Rabinowitsch-Mooney model and the Herschel Bulkley model used to calculate the apparent viscosity from the 4 g/liter fluid samples, illustrated with the blue line. For shear rates lower than 500 s^{-1} the estimated AV increases faster compared to the AV measured with the flow loop, but for higher shear rates there is almost a perfect fit. Some human error when reading of the Fann®35 values could result in an error like this. It can also be some error caused by the equipment, if it's not perfectly calibrated.

6.2.3 Back calculation

The back calculation results of the horizontal frictional differential pressure, presented in Fig. 5.33. indicates a decent relationship between the measured and calculated horizontal pressure drop. The largest difference in pressure drop is located around 60 - 70 l/min which can be a result of several factors. First of all it can be human error when reading of the shear readings with the Fann®35. This will result in wrong estimations of n, K and τ, which again will end up with dP_{hor} calculations that are slightly off. As the measured pressure drop from the flow loop are based on laminar and turbulent flow model only, the gap between the two slopes might be a result of the friction factor used to calculate the pressure drop for transient flow regime.

The estimated apparent viscosity values, shown in Fig. 5.34, are lower than the estimated values based on Equation (4.21), shown in Fig. 5.31. It is therefore concluded that the calculation method in section 4.2.2, based Rabinowitsch-Mooney equation are giving AV values closer to the true AV and that the back calculation method should not be used.

Chapter 7

Conclusion

7.1 Concluding remarks

To conclude this thesis, the instrumented standpipe concept looks promising based on the results from the flow loop tests. After adding the offset regression model to the differential pressure, the estimated density and apparent viscosity came close to their theoretical values, both for Newtonian and non-Newtonian fluid. It is also proven that the flow loop with the Rabinowitsch-Mooney calculation model agrees with theory for shear thinning Herschel Bulkley fluids.

The instrumented standpipe concept can bring several benefits to the drilling operations in the future. With live data of fluid density and viscosity in the well, the concept can deliver better estimation of ECD and thereby give better BHP control. This means that drilling can be done safer in narrow pressure windows. The live data will also contribute to a more time and cost efficient operation as the drilling crew can react faster as soon they see a change in the fluid properties in the well.

7.2 Future work

- Modify or change pressure sensors to get measurements closer to the actual flow.
- Test for different additives, and combinations of additives that reduces the bubble generation in the fluid.
- Install a pump with greater flow rate interval. Especially to deliver lower flow rates to compare with lower shear rates.
- Isolate the tank and install a heater to consider temperature effect on the fluid rheology.

References

[1] Caenn, R., Darley, H. C., and Gray, G. R. (2011). *Composition and properties of drilling and completion fluids*. Gulf professional publishing.

[2] Cengel, Y. A., Turner, R. H., and Cimbala, J. M. (2012). *Fundamentals of thermal-fluid sciences*.

[3] Djuve, J. and Hamre Vrålstad, J. (2015). *PET210 Øvinger i Bore- og Brønnvæsker*.

[Glossary] Glossary, S. *Picture of rheological models*. http://www.glossary.oilfield.slb.com/Terms/h/herschel-bulkley_fluid.aspx.

[5] Goswami, D. (2004). *The CRC Handbook of Mechanical Engineering, Second Edition*. CRC Press.

[6] Hjelm, O. A., Jøsang Nilsen, S., and Wærnes Vea, T. (2016). *Automatic Evaluation of Drilling Properties and Construction of Laboratory Model*. Faculty of Science and Technology, UiS.

[7] Kazan, B. and of Mechanical Engineers Shale Shaker Committee, A. S. (2005). *Drilling fluids processing handbook*. Gulf Professional.

[Klempa et al.] Klempa, M., Bujok, P., Jaroslav Struna, L. K., and Pinka, J. *Fundamentals of Onshore Driling*.

[9] Madlener, K., Frey, B., and H.K., C. (2009). *Generalized Reynolds number for non-Newtonian fluids*. EDP Sciences.

[10] Nguyen, Q.-H. and Nguyen, N.-D. (2012). *Continuum Mechanics - Progress in Fundamentals and Engineering Applications (Chapter 3)*. Intech.

[Ru] Ru, F. *Fann viscometer*. http://fann.ru/portfolio/fann-35/.

[12] Sui, D. (2017). *PET 525 Drilling Automation*. Not published. Used for lecturing.

[Wikipedia] Wikipedia. *Marsh funnel*. https://en.wikipedia.org/wiki/Marsh_funnel.

Appendix A

Matlab

The Matlab codes for the calculation methods are presented in Appendix A.

Fig. A.1. Code for estimation of water properties.

```
clear all
close all

Flowrate=xlsread ('measurements water ','C3:C37');
P_h=xlsread ('measurements water ','E3:E37');
P_v=xlsread ('measurements water ','F3:F37');
Density=xlsread ('measurements water ','H3:H37');

P_delta=P_v-P_h;  %calculates delta P from measured P_hor and P_ver values
P_delta_t=1000*9.81*3.5/100*ones(length(Density),1); %theoretical delta P for
water

offset=P_delta_t-P_delta;  %mBar offset between the measured and theoretical
delta P

figure
plot(Flowrate, Density)
grid
legend('Estimated density')
xlabel('Flowrate (l/min)')
ylabel('Density (kg/m^3)')
title('Density vs Flowrate')

figure
plot(Flowrate, P_delta,'r',Flowrate, P_delta_t,'b')
grid
legend('true measurement','theoritical values')'
title('Delta P vs Flowrate')
xlabel('Flowrate')
ylabel('P_v-P_h')

figure
plot(Flowrate, offset)
title('Offset')
xlabel('Flowrate (l/min)')
ylabel('Offset (mBar)')

grid

p=polyfit(Flowrate, offset, 6)  %polyfit function to make offset regression
model

offset_s=p(7)+p(6).*Flowrate+p(5).*Flowrate.^2+p(4).*Flowrate.^3+p(3).*Flowrat
e.^4+p(2).*Flowrate.^5+p(1).*Flowrate.^6;

figure
plot(Flowrate, offset,'r',Flowrate, offset_s,'b')
legend('Offset','Regression model of offset')
xlabel('Flowrate (l/min)')
ylabel('Offset (mBar)')
title('Offset vs Flowrate')


density_c=(P_delta+offset_s)/9.81/3.5*100; %Density after offset correction
grid
```

```
density_c=(P_delta+offset_s)/9.81/3.5*100; %Density after offset correction
grid

figure
plot(Flowrate, density_c,'r',Flowrate, density_c*0+1000,'b')
grid
legend('Estimated density','Density of water')'
xlabel('Flowrate (l/min)')
ylabel('Density (kg/m3)')
title('Fluid Density vs Flowrate')

density_c_l = lowpassFilter(density_c,1,10); %Density after offset correction
with low pass filter

figure
plot(Flowrate, density_c_l,'r',Flowrate, density_c*0+1000,'b',Flowrate,
density_c,'k')
grid
legend('Estimated density after filter','Density of waterv','Estimated density
before filter')
xlabel('Flowrate (l/min)')
ylabel('Density (kg/m3)')
title('Fluid Density vs Flowrate')
mean(density_c_l)

density_f=density_c_l;

D=0.024;            %inner pipe diamter
vis=1.002*10^-3;  %theoretical value apparent viscosity of water in room
temperature
A=pi/4*D^2;   %inner cross sectional area of pipe
e=10^-6;      %pipe roughness
L=3.5;          %distance between pressure sensors
vel=Flowrate/60000/A;   %fluid velcity
vis=1.002*10^-3;
rho=1000;           %water density

f_e=P_h*100*2*D./density_f'/L./vel./vel;
f_o=(P_h-14)*100*2*D./density_f'/L./vel./vel;

Re_t=rho*D.*vel/vis;
for i=1:length(Re_t)
    if Re_t(i)<=2300
        f(i)=64/Re_t(i); %Darcy-Weisbach friction factor
    else
       f(i)=1/(-1.8*log10((e/D/3.7)^1.11+6.9/Re_t(i)   ))^2;
%        %Haaland's friction factor
    end
end
```

```
figure
plot(Flowrate, f_e,'r',Flowrate, f,'k',Flowrate, f_o,'b')
legend('estimated f before offset','true f','after offset')
xlabel('Flowrate (l/min)');
ylabel('Friction factor');
title('Friction Factor vs Flowrate');
grid

Re_e=64./f_o;
weight=0.01;
for i=1:length(Re_e)
    if Re_e(i)>2000
        Re_e(i)=6.9/(10^(-1/1.8./sqrt(f_o(i)))-(e/D/3.7)^1.11);
    end
    if Re_e(i)<2000&&Re_e(i)>1000
        Re_e(i)=weight*64/f_o(i)+(1-weight)*6.9/(10^(-1/1.8./sqrt(f_o(i)))-
(e/D/3.7)^1.11);
        temp=1;
    end

end
figure
plot(Flowrate, Re_e,'r',Flowrate, Re_t,'k')
legend('Measured value','Theoretical value')
title('Reynolds number vs flowrate')
xlabel('Flowrate (l/min)')
ylabel('Re')
vis_e=vel.*density_f'*D./Re_e;
 vis_e=lowpassFilter(vis_e,1,20)'; %low pass filter added
 min(vis_e)

figure
plot(Flowrate, vis_e,'r',Flowrate, vis_e*0+vis,'k')
legend('Measured value','Theoretical value')
title('Viscosity vs flowrate')
xlabel('Flowrate (l/min)')
ylabel('Viscosity')
```

Fig. A.2. Code for density estimation of Duotech NS fluid.

```
clear all
close all

% Flowrate=xlsread ('flow loop duotech NS','3 g-l','C4:C36');
% P_h=xlsread ('flow loop duotech NS','3 g-l','D4:D36');
% P_v=xlsread ('flow loop duotech NS','3 g-l','E4:E36');
%
% Flowrate=xlsread ('flow loop duotech NS','5 g - l','C4:C35');
% P_h=xlsread ('flow loop duotech NS','5 g - l','D4:D35');
% P_v=xlsread ('flow loop duotech NS','5 g - l','E4:E35');

Flowrate=xlsread ('flow loop duotech NS','4 density','C12:C25'); %reads values
from excel sheet
P_h=xlsread ('flow loop duotech NS','4 density','D12:D25');      %from row 12
to 25
P_v=xlsread ('flow loop duotech NS','4 density','E12:E25');

P_delta=P_v-P_h;  %delta P between horizontal and vertical diff. pressure
P_delta_t=1000*9.81*3.5/100*ones(length(P_h),1);


load offset_co.mat

offset_s=p(7)+p(6).*Flowrate+p(5).*Flowrate.^2+p(4).*Flowrate.^3+p(3).*Flowrat
e.^4+p(2).*Flowrate.^5+p(1).*Flowrate.^6;
%offset based on diff p data

figure
plot(Flowrate, P_delta,'r',Flowrate, P_delta_t,'b')
grid
legend('true measurement','theoretical values water')'
xlabel('Flowrate (l/min)')
ylabel('P_v-P_h (mBar)')
title('dP vs Flowrate, Duotech NS 4 g/l')

figure
plot(Flowrate, offset_s)
xlabel('Flowrate (l/min)')
ylabel('Offset (mBar)')
title('Offset vs Flowrate')
grid

density_c=(P_delta+offset_s)/9.81/3.5*100;  %Density after offset correction
grid

figure
plot(Flowrate, density_c,'r-*',[85, 70, 50, 38,25,10],
[.935,0.929,.94,.941,.944,.95]*1000,'b*');
%vectors from drilling fluid laboratory tests. flowrates in vector 1,
%and densities in vector 2
grid
legend('Estimated density of 4 g/l Duotech NS','Density of 4g/l Duotech NS
(laboratory')
xlabel('Flowrate (l/min)')
ylabel('Density kg/m^3')
title('Fluid density vs Flowrate')
```

```
density_c_l = lowpassFilter(density_c,1,3); %Offset corrected density with low
pass filter

figure
plot(Flowrate, density_c_l,'r',Flowrate, density_c*0+1000,'b',Flowrate,
density_c,'k')
grid
legend('Estimated density after filter','Density of water','Estimated density
before filter')
xlabel('Flowrate (l/min)')
ylabel('Density kg/m^3')
title('Filter effect')

mean(density_c_l)
```

Fig. A.3. Code for apparent viscosity estimation of Duotech NS fluid.

```
clc
clear
% close all


%% inputs
Flowrate=xlsread ('flow loop duotech NS','3 g-l','C4:C36');
P_h=xlsread ('flow loop duotech NS','3 g-l','D4:D36');
P_v=xlsread ('flow loop duotech NS','3 g-l','E4:E36');
%
Flowrate3=xlsread ('flow loop duotech NS','5 g - l','C4:C35');
P_h3=xlsread ('flow loop duotech NS','5 g - l','D4:D35');
P_v=xlsread ('flow loop duotech NS','5 g - l','E4:E35');
%
Flowrate4=xlsread ('flow loop duotech NS','4 density','C12:C25');
P_h4=xlsread ('flow loop duotech NS','4 density','D12:D25');
P_v=xlsread ('flow loop duotech NS','4 density','E12:E25');

R=0.012;

Q=Flowrate/60000;    % 3 g/l (m^3/s)
Q3=Flowrate3/60000;%5 g/l
Q4=Flowrate4/60000;%4 g/l
A=pi*R^2;

v=Q/A; %3 g/l
v3=Q3/A; %5 g/l
v4=Q4/A; %4 g/l

DP=(P_h-14)*10^2;
DP3=(P_h3-14)*10^2;
DP4=(P_h4-14)*10^2;
L=3.5;

tau=2*R*DP/4/L; %Wall shear stress      3g/l
tau3=2*R*DP3/4/L;  %5g/l
tau4=2*R*DP4/4/L;  %4 g/l

%Define y and x as in section 4.2.3
y=log(tau);
x=log(4*v/R);     % 4v/R= (8u/D)

y3=log(tau3);      %5 g/l
x3=log(4*v3/R);

y4=log(tau4)      %4 g/l
x4=log(4*v4/R)

for i=1:length(x)-1
 gr(i)=(y(i+1)-y(i))/(x(i+1)-x(i)); % gr = n
 r_w(i)=(3*gr(i)+1)/4/gr(i)*4*v(i)/R; % shear rate at wall

 vis_a(i)=tau(i)/r_w(i);   %Apparent viscosity for 3 g/l
end
```

```
for i=1:length(x3)-1
 gr3(i)=(y3(i+1)-y3(i))/(x3(i+1)-x3(i)); % gr = n
 r_w3(i)=(3*gr3(i)+1)/4/gr3(i)*4*v3(i)/R;

 vis_a3(i)=tau3(i)/r_w3(i);  %5 g/l
end

for i=1:length(x4)-1
 gr4(i)=(y4(i+1)-y4(i))/(x4(i+1)-x4(i)); % gr = n
 r_w4(i)=(3*gr4(i)+1)/4/gr4(i)*4*v4(i)/R;
    %4 g/l try 2
 vis_a4(i)=tau4(i)/r_w4(i);   %4 g/l
end

theta=[600 300 200 100 6 3];  %RPM
readings=[28.9 22.5 19.94 16.4 9.98 9.06];% shear readings for 4 g/l

shear_r=1.7023*theta; %shear rate
shear_s=1.067*readings*0.4788; %shear stress
vis_a1=shear_s./shear_r; %apparent viscosity from drilling fluids laboratory

figure
plot(shear_r, vis_a1,r_w,vis_a,'o',r_w3,vis_a3,'*',r_w4,vis_a4,'o');
title('Apparent Viscosity vs Shear rate - Duotech NS 4 g/liter')
xlabel('Shear rate (s^{-1})')
ylabel('Apparent Viscosity (Pa*s)')
legend('AV Duotech NS laboratory','Flow loop measurements 3 g/l',...
'Flow loop measurements 5 g/l','Flow loop measurements 4 g/l')
```

Fig. A.4. Code for back calculation of horizontal differential pressure drop and apparent viscosity.

```
clc
clear

r_pi = 0.024/2;                          %drillpipe internal radius [m]
D=2*r_pi;                                %Internal diameter
flow=xlsread ('flow loop duotech NS','4 density','C12:C25')/60000;
rho_f = 948;       %average density of mud based on low pass filter
L=3.5;             %length between pressure sensors
A=pi*r_pi^2;        %internal cross section area
vel=flow/A;         %fluid velocity
e=0.001;            %pipe roughness
f_guess = 0.005;    % guessed friction factor

%% Calculation of HB-parameters
theta=[600 300 200 100 6 3];             %RPM
readings=[28.9 23 19.9 17 10.5 9.5];%4   shear readings
shear_r=1.7023*theta;           %shear rate [s^{-1}]
shear_s=1.067*readings*0.4788;  %shear stress
mu_t=shear_s./shear_r;

x0 = [0,0,0];
x = fsolve(@(x) HB_parameters(x,shear_s,shear_r),x0);

Tau_0 = 4.1902;  %estimated yield stress from shear readings
K = 0.25099799;  %estimated K from shear readings
n = 0.54056838;  %estimated n from shear readings

for i=1:length(vel)
    m(i)=n*K*(8*vel(i)/D)^n/(Tau_0+n*K*(8*vel(i)/D)^n);%generalized flow index
    Re(i)=rho_f*(vel(i))^(2-n)*D^n/(Tau_0/8*(D/vel(i))^n...
        +K*((3*m(i)+1)/(4*m(i)))^n*8^(n-1));  %generalized HB Reynolds number
    D_eff(i) = D_eff_dp(m(i),r_pi);              %effective diameter
    f(i) = ff_d(e,D_eff(i),m(i),Re(i),f_guess);  %calls on friction factor
function
    dpdx(i) = dpdx_dp(f(i),rho_f,flow(i),r_pi)*L;  %differential pressure drop
in horizontal pipe
    mu_a(i)=rho_f*vel(i)*D_eff(i)/Re(i);     % apparent viscosity estimated
from generalized Herschel Bulkley number with (Equation (2.18))
    sh_r(i)=8*vel(i)/D*(3/4+1/4*m(i));      %shear rate from Equation (4.17)

end

P_h=xlsread ('flow loop duotech NS','4 density','D12:D25');
figure(1)
plot(flow*60000,(P_h-14),'r',flow*60000,dpdx/100,'b')
title('Measured vs Estimated Frictional Pressure Drop');
xlabel('Flow rate (l/min)');
ylabel('dP_{hor} (mBar)');
legend('Measured dP_{hor}','Estimated dP_{hor}')

figure
plot(sh_r,mu_a,'r*',shear_r,mu_t,'b')
axis([0 1200 0 0.04])
title('Apparent Viscosity vs Shear rate - Back calculation')
xlabel('Shear rate (s^{-1})')
ylabel('Apparent viscosity (Pa.s)')
legend('AV from from Re_{HB-gen}', 'AV Duotech NS laboratory')
```

Appendix B

Simulink

Fig. B.1. Illustration of live data before stabilized flow.

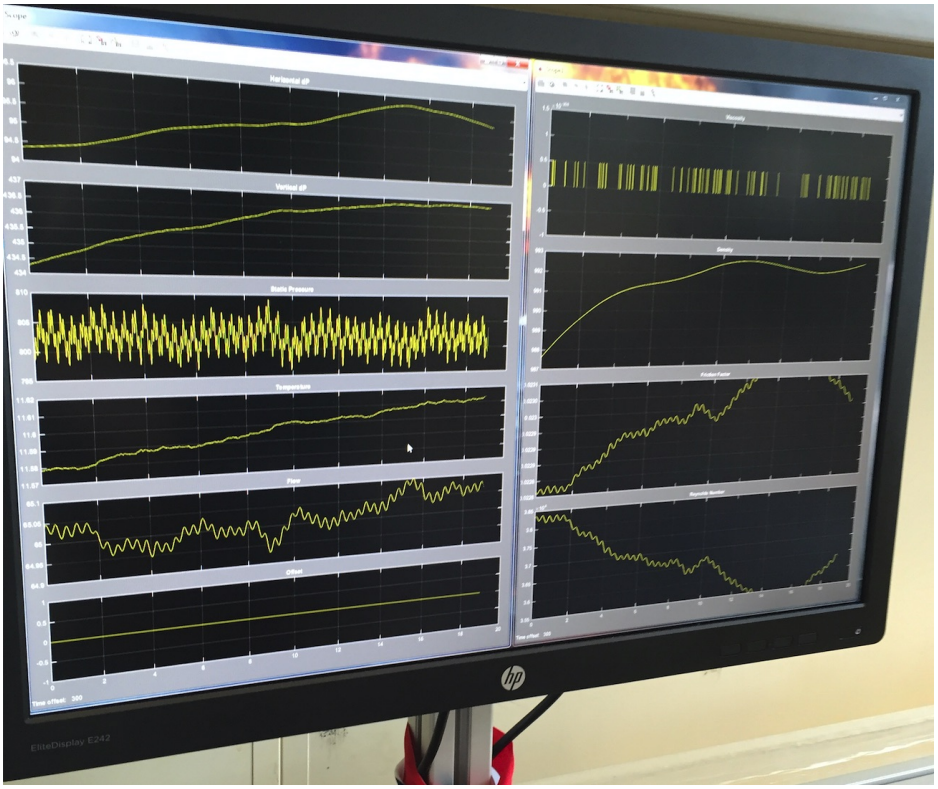

The window to the left shows how vertical dP, horizontal dP, static pressure, temperature and flow rate variates with time during start up of the flow loop. The window to the right illustrates estimated viscosity, density, friction factor and Reynolds number with time.

Fig. B.2. Simulink structure.

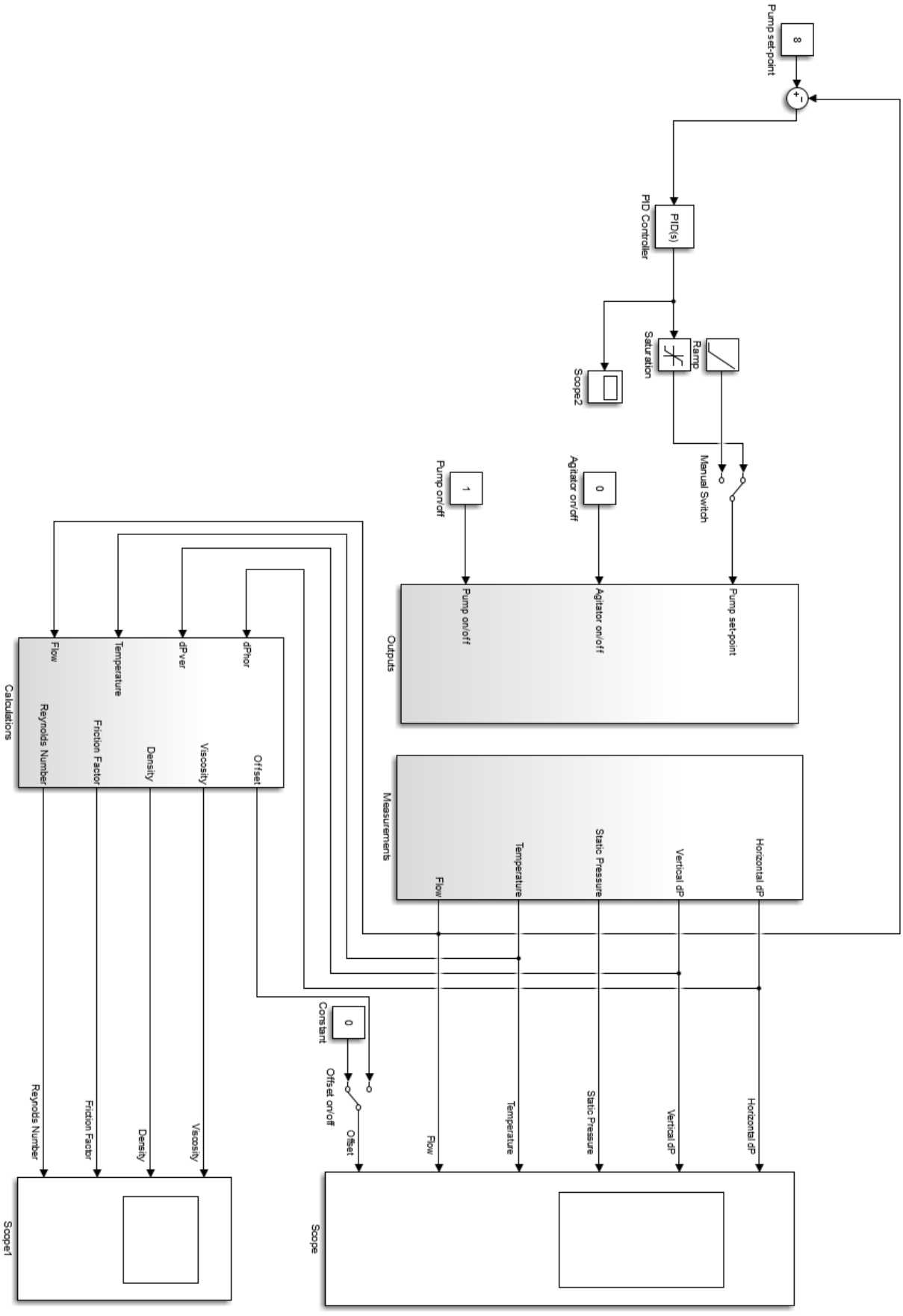

Appendix C

Excel measurements

Fig. C.1. Flow rate and differential pressure measurements for water.

	Measured Flow rate	dP Horizontal	dP Vertical
1	89,99	166,0235	513,3786
2	86,9808	157,168	503,0674
3	81,9985	143,2224	486,4625
4	76,9712	126,0292	466,5053
5	75,0007	121,7084	461,5119
6	69,9943	109,4954	448,0328
7	64,0176	95,8791	432,0901
8	59,9831	87,0895	422,3668
9	55,0078	76,8623	410,6043
10	49,9871	66,8772	399,252
11	44,9813	58,4425	389,4788
12	40,0006	51,6745	381,9175
13	34,9983	42,0807	371,9059
14	29,9947	35,1927	363,9524
15	27,9998	31,7332	361,0886
16	26,9912	32,2639	360,6631
17	26,0098	32,056	360,8884
18	24,9996	29,4926	357,5402
19	24,0313	27,856	355,8211
20	22,9882	27,9375	355,7596
21	21,9135	26,8951	354,6038
22	20,9882	25,8682	353,0458
23	20,0066	24,9141	352,028
24	18,9862	23,9998	350,7151
25	16,994	22,3022	348,6188
26	16,0078	21,7659	347,8275
27	14,0028	20,107	345,9331
28	11,9371	18,6196	344,2898
29	9,9611	17,4387	342,7791

Fig. C.2. Flow rate and differential pressure measurements for Duotech NS 4 g/liter batch.

	Xanthan gum (Duotech NS) 4g/liter		
	measured flowrate	dP Horizontal	dP Vertical
1	85,1028	127,8752	455,5026
2	80,0017	117,6335	442,3947
3	69,9781	111,415	431,3855
4	60,0327	102,5865	418,8672
5	50,0031	95,5874	407,8311
6	46,0128	91,3223	403,2379
7	42,0485	88,1043	399,1102
8	37,9963	84,74	394,2419
9	33,9268	81,0082	390,5413
10	29,9113	77,6428	387,2223
11	25,002	73,4883	385,0037
12	19,9309	68,3944	381,2472
13	14,9974	64,1581	378,7706
14	10,0054	59,1161	375,9132